Hindawi
Journal of Advanced Transportation
Volume 2024, Article ID 3835831, 21 pages
https://doi.org/10.1155/2024/3835831

WILEY | Hindawi

Research Article

Investigating the Impact of Automated Vehicles on the Safety and Operation of Low-Speed Urban Networks

Amir Hossein Karbasi,[1] **Nan Zheng**,[2] **and Steve O'Hern**[3,4]

[1]*Department of Civil Engineering, McMaster University, Hamilton, ON, Canada*
[2]*Monash University, Institute of Transport Studies, Clayton, VIC 3800, Australia*
[3]*Institute for Transport Studies, University of Leeds, Leeds, UK*
[4]*Monash University Accident Research Centre, Clayton, VIC 3800, Australia*

Correspondence should be addressed to Nan Zheng; nan.zheng@monash.edu and Steve O'Hern; s.ohern@leeds.ac.uk

Received 13 November 2023; Revised 19 February 2024; Accepted 16 March 2024; Published 27 March 2024

Academic Editor: Giuseppe Musolino

Automated vehicles (AVs) will appear on the road soon and will influence the properties of road traffic networks such as capacity and safety. While the impact of AV on traffic operations has been discussed extensively, most existing literature in this direction focuses on microscopic and mesoscopic levels. This study examines the effect of AVs on traffic flow operations and crash risks at a network scale. In addition, this study discusses the implications for designing and operating safe, low-speed urban road networks. Simulation experiments were carried out in a grid road network with AVs and human-driven vehicles operating in mixed flow conditions. To assess traffic performance, the macroscopic fundamental diagram (MFD) relationships were estimated, specifically focusing on speed-density correlations. From this analysis, it was possible to extract key traffic performance indices such as capacity and critical speed. Using time-to-collision surrogate safety measures, macroscopic safety diagrams were generated which associate the level of congestion with the potential crash conflicts among vehicles at an aggregated spatial scale. Utilizing this knowledge, a novel multiobjective optimization based on the NSGA-II algorithm was applied to identify the optimal trade-off between efficiency and safety. The presence of AVs was found to have a positive impact on the capacity, critical density, and average speed on a system level, even in low-speed scenarios. Moreover, AVs can result in increased critical density in the network, which suggests that the road system can serve more vehicles at its capacity, thus improving efficiency, while decreasing the number of conflicts. These findings are useful for both traffic planners and operators.

1. Introduction

Transportation networks face many challenges such as high travel times, traffic congestion, crashes, and environmental externalities such as emissions [1–4]. Congestion is the root of other problems such as increased fuel consumption and increased travel time. For example, in 2021 American drivers lost an average of 36 hours per year due to traffic congestion [5]. Meanwhile, the U.S. Department of Transportation's National Highway Traffic Safety Administration report [6] found that over twenty thousand people lost their lives in motor vehicle crashes in the first half of 2021, up 18.4% over the first half of 2020. Therefore, it is necessary to find solutions to improve the safety and decrease traffic congestion.

Due to the advancement of technology, it is predicted that automated vehicles (AVs) may help reduce congestion and improve safety [7–9]. From a traffic flow viewpoint, AVs can benefit from smaller headway due to automation features [10, 11]. Thus, AVs are expected to have a positive effect on congestion mitigation. From the safety point of view, human error is a contributing factor in up to 90 percent of crashes [12, 13], and AVs are believed to significantly reduce the risks and consequences of crashes [14–20].

Many studies have investigated the impact of AVs on traffic flow and safety in different environments and situations [11, 16, 20–26]. Some of these studies have explored the impact of AVs on fundamental diagrams (MFDs) and the capacity of transportation networks [10, 27, 28]. On the other hand, others have investigated the safety impact of AVs based on safety measures [16, 20, 21, 26, 29]. However, to our knowledge, no studies have yet investigated the impact of AVs on MFDs and safety simultaneously. Moreover, these studies have not explored the impact of AVs on macroscopic safety diagrams (MSDs) a concept introduced by Alsalhi et al. [30]. MSDs share a conceptual foundation with MFDs, indicating that, like MFDs—which propose that traffic flow is a function of traffic density—MSDs can also apply this concept, making them essentially a function of density [30]. Thus, generally, MSDs show the relationship between traffic conflicts and density. However, given the conflicts between speed, flow, and safety [31, 32], it is not clear to what extent AVs can affect the conflicts between flow and safety.

Thus, to fill these gaps, this study investigates the impact of AVs on network performance as measured through the simultaneous analysis of MFDs and MSDs. The case study is a grid network with 50 km/h and 30 km/h speed limits. The primary motivation for choosing a grid network as a low-speed urban network is that the safety issues for intersections are crucial because many accidents occur at intersections. For example, 43 percent of traffic crashes involve intersections in the United States [33]. Moreover, this study analyzes the impact of AVs on stop-and-go waves which are a common occurrence at intersections [20]. Furthermore, this study presents a novel framework in which multi-objective optimization finds a set of solutions in which traffic flows are high and the number of crashes remains low. At the end of this study, a comparison is made between urban speed limits based on the MFDs and MSDs. The main contributions of this study are below:

(1) Investigating the impact of AVs on traffic flow and safety simultaneously based on macroscopic and microscopic analysis.

(2) Presenting a multi-objective optimization maximizing traffic flow while minimizing conflicts.

(3) Comparing two urban speed limits based on MFDs and MSDs in the presence of AVs.

The remainder of the paper is organized as follows. Section 2 provides a review of previous studies on the effects of AVs on MFDs and safety. The review highlights the unique contribution of this study. Section 3 presents the methodology for the study including the macrosimulation networks, car-following models, the method for generating MFDs and MSDs, safety analysis methods, and multi-objective optimization utilized. Section 4 displays the results obtained from the simulations. Finally, Section 5 presents the discussion and conclusion.

2. Literature Review

The potential impact of AVs and connected and automated vehicles (CAVs) on traffic operations in road networks has been studied extensively. We do recognize the existence of a large body of work in this area, this review selects representative works for gap identification and discussion purposes. The review is presented in two parts. First, we discuss key studies that have investigated the impact of AVs on traffic operations, focusing on traffic performance modeling at different scales under AV influences. Second, we discuss studies that have addressed the issue of the safety impact of AVs.

2.1. Impact of AVs on Traffic Flow. The modeling of traffic flows is one of the key functions of traffic engineering [34]. aggregate traffic flow modeling techniques. In particular, the MFDs have been studied and applied to network-level analysis, where an MFD relates the vehicle accumulation in a road network (e.g., the total amount or density of vehicles which reflects "traffic state" or "level of congestion" of the network) to the trip completion rate (e.g., the amount of trips completed in the network which reflects "level of service" or "efficiency" of the network).

The simple form of the MFD was first introduced by Godfrey [35], and then Mahmassani et al. [36] and Daganzo [37] enhanced this notion. Moreover, Geroliminis and Daganzo [38] and Geroliminis and Sun [39–42] demonstrated empirically and through simulation experiments that well-defined MFDs exist for large-scale urban traffic networks. Given this unique feature, the MFD has been applied for neighborhood- or network-level demand and operation management, such as congestion pricing (e.g., [43, 44], traffic signal control (e.g., [45, 46], and road space allocation (e.g., [47, 48].

While the existence of MFDs was demonstrated in networks of conventional vehicles, further studies have investigated the properties of MFDs when other types of vehicles are available to users and operated in a shared space. For instance, Shelton [25] carried out a study using a multiresolution model and highlighted how the network capacity can be increased when the penetration rate of AV increases from 0% to 100%. Ghiasi et al. [22] proposed a Markov-chain-based analytical model, which estimated the change in headway when vehicles formulate platoons and analyzed the performance of traffic flow under variations in platooning and CAV penetration rates. The research findings revealed that the capacity could be increased when CAV penetration rate and platoon intensity increase in mixed traffic for freeway operation scenarios.

On a smaller scale, Martin-Gasulla et al. [24] carried out a study to investigate how CAVs can change the capacity at a signalized intersection. They identified the importance of high penetration rates of CAVs for maintaining throughput. Liu and Fan [11] applied the Wiedemann car-following

model [49] for human drive vehicles (HDVs), which is calibrated using real data to evaluate CAVs effect on the capacity of a freeway. They also developed a revised intelligent driver model (IDM) to account for the features of CAVs. Their analysis indicated that freeway capacity increased 85% when CAV penetration rate was 100% when operating in a 65mph (104 km/h) speed zone. Xiao et al., [28] examined the impact of cooperative adaptive cruise control (CACC)-equipped vehicles on the capacity and capacity drop at merging bottleneck based on CACC systems. Xiao et al. [28] found that the capacity of a merging section can be increased by nearly 60% when the penetration rate of CACC equipped vehicles is 100%.

Initial attempts emerged at measuring the impacts of AVs on large-scale traffic operations, measured such as the road capacity of a network. For instance, Atkins [10] employed the Wiedemann 99 car-following model for a simulation-based analysis and showed that the inclusion of CAVs has a positive impact on capacity, e.g., the maximum flow observed on the MFDs is higher when the penetration rate of CAVs increases. Talebpour and Mahmassani [27] proposed a framework to evaluate the impact of CAVs and AVs on traffic flow. The results based on MFDs suggested that throughput improves when the penetration rate of connected vehicles (CVs) and (AVs) increases; however, AVs were found to increase throughput more than CVs.

While many studies indicate that AVs will have a positive influence on traffic efficiency, other research suggests they may have a negative effect on traffic flow [50–52]. Whether AVs have a positive or negative effect varies depending on a range of factors included their level of automation, the technologies incorporated into the AV, driving behavior, uptake, and permeation into the vehicle fleet. This conjecture highlights the need for further research to understand the scenarios where AVs can have a positive influence on traffic network performance, which can ultimately assist in guiding AV policy.

2.2. Impact of AVs on Traffic Safety. AVs and CAVs have the potential to eliminate many common human errors (such as speeding and distracted driving) associated with crashes, as such, AVs are expected to improve safety substantially (Manivasakan et al., 2021, Zou et al. 2021). Many studies have attempted to estimate the reduction in crashes due to AVs. These studies have used different surrogate safety measures (SSMs) show to the extent to which AVs can improve traffic safety in different environments and under different driving conditions.

Investigating the benefits brought by AVs and CAVs is a classical and well-studied topic. For example, Virdi et al. [20] demonstrated the improved safety at intersections and highways as the CAVs were controlled under a so-called "Virdi CAV Control Protocol" in a mixed traffic flow environment. The work illustrated that when the penetration rate of CAVs is over 80%, conflicts could decrease substantially. Karbasi and O'Hern [23] tested an even higher penetration rate of 100% AVs and CAVs for intersection scenarios and found further reduction. Similar conclusions can be found in other studies as well, e.g., Papadoulis et al. [16] and Arvin et al. [21]. Interestingly, the safety impact of AVs/CAVs is not always found to be positive. Papadoulis et al. [16] identified that certain types of crashes did not benefit from the CAV operations; for example, an increased number of read-end conflicts were observed. This is reasonable because the AVs/CAVs tend to operate at smaller headways, resulting in closed space between the vehicles and smaller TTC. In a large network where AVs/CAVs and HDVs operate in a shared space, the safety benefits or crash risks obviously are not spatially homogeneous. While it is important to identify where the black spots are located, there is a need to understand the system level of safety. Further research by Sinha et al. [17] evaluated the crash severity and rate of conventional vehicles in mixed fleets with connected and automated vehicles. In addition, Dixit et al. [14] performed a safety and risk analysis of autonomous vehicles using computer vision and neural networks.

Generally, despite the studies using different approaches, methods, and road networks, the findings show that AVs have the potential to improve safety and reduce congestion. However, most existing studies did not consider the correlation between safety and traffic congestion. It is sensible to examine the traffic-dependency feature of vehicle operation safety. This will be particularly useful for AV analysis, as it enables a holistic understanding of AV benefits and costs. The challenge though, lies in the fact that high flow and low crash are too conflicting objectives. To this end, there is the potential to identify a set of points where optimal trade-offs can be made. The first work on this research direction was reported in Alsalhi et al. [30] who argued a relationship between crash risks and traffic density, namely, the macroscopic safety diagram (MSD). Interestingly, the MSD has a similar shape to MFDs but a higher "critical density" where the crash risk appeared to be the lowest (as compared to the MFD case, the maximum flow is achieved at its "critical density"). The MSD is a single mode model, not yet applicable for multi-modal traffic environment such as a mixed HDVs and AVs system. It is expected that AV-involved MSD will exhibit new patterns, given its unique operation characteristics.

To summarize, this paper aims to address some of the previous methodological limitations by examining the impact of AVs on MFDs and MSDs, identifying optimal operation solutions for safety-efficiency trade-offs, and offering the relevant insights on policy indications. Concerning policy demonstration, this paper conducts a case study on the impact of influencing speed limits in a road traffic network involving autonomous vehicles (AVs).

3. Methodology

To obtain extensive scenarios for the targeted AV impact analysis, this study carries out a simulation-based analysis. The employed simulation, SUMO [55], is based on microscopic traffic flow models, i.e., the car-following models, which define the driving behavior of HDVs and AVs. Six scenarios for AV penetration were considered with the percentage of AVs increasing market penetration rate

(MPR) by 20% between 0% and 100%. This study performs a simulation on a grid road network that includes nine intersections. To generate MFDs based on simulation data, the Papageorgiou speed-density model [56] is used, and capacities, average speed, and critical densities based on different scenarios are determined. To investigate the safety impact of AVs, the time to collision (TTC) surrogate safety measure (SSM) is used to determine conflicts between vehicles. MSDs are generated using a second-degree equation which is based on the relationship between conflicts and densities. To find a set of solutions in which the flow is high and conflicts are low, a multiobjective optimization based on the NSGA-II genetic algorithm is presented with the optimization based on minimizing the second degree equation and maximizing the network-level traffic flow. The case study uses hypothetical demands to reflect different degrees of congestion within a grid network.

The methodology of this paper is presented in four steps. First is the microsimulation in which driver behavior of AVs and HDVs is defined. The second step is generating MFDs which are based on simulation data and speed-density models. In the third step, safety analysis based on TTC is presented, and MSDs are constructed based on safety outputs. The second-degree relationship between density and the number of conflicts is also presented. In the last step, a multiobjective optimization problem is formulated, and the solution algorithm is introduced, in which based on the density-velocity model and the tertiary safety relationship, optimal points are found in which not only the flow is high but also the number of TTC incidents is low.

3.1. Microsimulation. To define the vehicle behavior of HDVs and AVs in microsimulation, a set of longitudinal and lateral equations based on car-following models and lane-changing models is required. The SUMO simulator was used to simulate the driver behavior of HDVs and AVs in this study. This study uses the Weidmann model for HDVs and the intelligent driver model (IDM) for AVs to reflect their distinct driving behaviors. The Weidmann model was selected for its precise representation of human driving behaviors, while the IDM was chosen for AVs to showcase the benefits of automation in terms of safety and efficiency. Parameters for both AV and HDVs are based on the study by Atkins [10]. The AVs parameters are based on the level IV definition given by Atkins [10], meaning that the vehicles are operating without a human driver.

The longitudinal driving behavior of HDVs was defined using the Wiedemann 99 car-following model. Based on the perceptions of relative speed and position changes by the following driver, Wiedemann's model determines the following driver's reactions, such as acceleration or deceleration [57]. Four parameters of this car-following model are used to define driving behavior at intersections. The definition of these parameters and the values used in this study are presented in Table 1.

To define the AVs' longitudinal driving behavior, the intelligent driver model (IDM) car-following model, developed by Treiber et al. [58], was used. IDM calculates acceleration by measuring two ratios: desired velocity and actual velocity and desired headway and actual headway [11, 23]. Equations (1) and (2) show the calculation of acceleration:

Table 1: Wiedemann 99 car-following parameters.

Parameter	Unit	Description	Value
CC0	m	Standstill distance	1.5
CC1	s	Spacing time	0.9
CC7	m/s^2	Oscillation acceleration	0.25
CC8	m/s^2	Standstill acceleration	3.5

$$a = a_0\left(1 - \left(\frac{v}{v_0}\right)^{\delta} - \left(\frac{s^*(v,\Delta v)^2}{s_0}\right)^2\right), \tag{1}$$

$$s^*(v,\Delta v) = s_0 + \max\left(0, vT + \frac{v\Delta v}{2\sqrt{a_0 b}}\right), \tag{2}$$

where a and a_0 are acceleration and maximum acceleration, v and v_0 are current speed and desired speed, respectively, δ is the acceleration exponent, $s^*(v,\Delta v)$ is desired minimum headway, s_0 is current headway, T is the desired headway, b is deceleration, Δv is the difference in speed between the lead and following vehicle. For AVs, the desired time headway is equal to 0.5 s, the minimum gap is equal to 0.5 m, and maximum acceleration is 3.8 m/s^2, as reported by Atkins [10]. This study used the SUMO simulator default lane-changing model called LC2013 [59] for both HDVs and AVs to capture lateral movements of vehicles and intersection movements. SUMO includes three lane-changing motivations: strategic, cooperative, and tactical lane-changing. For this study, strategic lane changing was used, which initiates lane changing when the vehicle finds no connection between the current lane and the next lane on the route [29].

3.2. Quantifying the Network-Level Traffic Flow Operation: The Macroscopic Fundamental Diagrams. MFDs represent the relationship between flow, density, and speed and are often represented as flow density and speed-density diagrams. The MFD presents information on traffic characteristics, such as the value of free-flow speeds and flow capacities. The MFD can be used to distinguish between free-flow and congested traffic conditions. The relationship between flow, density, and speed is shown in the following equation:

$$Q_i(p_i) = V(p_i).\, p_i, \tag{3}$$

where $Q_i(p_i)$ is flow, p_i is average density, and $V(p_i)$ is speed (km/h). In this study, to generate MFDs from microsimulation data, a speed-density model is used. The speed-density model is used because there needs to be a relationship between flow and density for a multi-objective optimization formulation. Therefore, by using the speed-density model and substituting it into equation (3), a mathematical formula for the relationship between flow and density can be obtained. This study uses Papageorgiou speed-density model [56] which provides information such

as free-flow speed and critical density (the point at which the flow reaches its highest value). The following equation shows the Papageorgiou speed-density model [56] relationship:

$$V(k) = v_f \exp\left[\frac{-1}{a}\left(\frac{p}{p_c}\right)^a\right], \tag{4}$$

where v_f is free-flow speed, p_c is critical density, p is density, and a is the model shape parameter. By substituting (4) in (3), the relationship between flow and density is obtained. This study uses SUMO edge-based output data [59]. In SUMO, edge-based data provide traffic metrics as outputs including average speed and density for each network edge at varying time intervals (e.g., every 60 seconds). A detailed description of this feature in SUMO is available in SUMO [59]. To aggregate this data for the network and generate MFDs based on edge-based output data, the macrOutput.py tool was used [60].

3.3. Quantifying the Network-Level of Crash Risks: The Macroscopic Safety Diagram. In dynamic urban networks, MSDs aim to explore the possible relationship between safety performance (e.g., the likelihood of a multi-vehicle rear-end collision) and operational performance (e.g., traffic conditions at that time) [30]. This study uses MSDs to show the relationship between the number of conflicts and density.

Before explaining the MSDs, it is necessary to define the definition of the conflict based on safety measures. In this study, TTC is used to determine conflicts. If two vehicles followed their current path and maintained their current speed, TTC would be the remaining amount of time before a collision occurred [61, 62]. In the SUMO simulator, SSM device output [59] is used to generate conflicts based on TTC safety measures. SSM devices generate outputs including type of conflicts, positions of vehicles, and TTC value. In the SSM device, the TTC is calculated in the following two ways:

$$\mathrm{TTC} = \frac{\left(\left(x_{i-1,t} - x_{i,t}\right) - L_{i-1,t}\right)}{v_{i,t} - v_{i-1,t}}, \tag{5}$$

$$\mathrm{TTC} = \frac{x_{i,t}}{v_{i,t}}, \tag{6}$$

where $x_{i-1,t}$ is the leader position at the time t, $v_{i-1,t}$ is the leader speed at the time t, $x_{i,t}$ is the position of the following vehicle and $v_{i,t}$ is the speed of the following vehicle at the time t, $L_{i-1,t}$ is the length of vehicle at the time t. (5) calculates rear-end collisions, and (6) calculates merging and crossing conflicts. This study uses two different TTC threshold values for HDVs and AVs. The TTC threshold is used to identify potential conflicts, i.e., when maneuvers occur below the threshold value. The TTC threshold value for HDVs is 1.5 s which has been suggested in previous studies [16, 20, 63]. Previous research has demonstrated that the minimum gap for AVs is one-third of the minimum gap for HDVs, and as such a TTC threshold of 0.5 s was selected [20].

Based on safety and density outputs, MSDs were generated using a nonlinear regression to fit a simple second-degree polynomial model to the simulation data which present the relationship between conflicts and density:

$$\mathrm{PC} = a.p_i^2 + b.p_i, \tag{7}$$

where PC is the number of potential conflicts and a and b are the equation parameters. Critical density associated with maximum conflicts is obtained by finding the roots of the equation (7). The critical conflict point (*CCP*) is obtained by substituting the critical density into (7), which has been shown in the following equation:

$$\mathrm{CCP} = a.(\mathrm{CD})^2 + b.\mathrm{CD}, \tag{8}$$

where CCP is the peak conflict in a period and CD is the critical density associated with maximum conflicts. Similar to MFDs, (7) is necessary because there needs to be a relationship between the number of conflicts and density for a multiobjective optimization formulation.

3.4. The Efficiency-Safety Trade-Off through a Multiobjective Optimization. As mentioned before, there is a contradiction between flow and crashes in that the probability of a crash increases as the flow increases and moves towards the capacity of the road [30]. Therefore, there is a trade-off between flow and safety. Therefore, it is essential to pursue a multi-objective optimization approach that identifies scenarios where both the flow-to-capacity ratio is maximized and the conflict-to-maximum-conflict ratio is minimized, ensuring an optimal balance between traffic efficiency and safety. In this study, there are two objective functions. The first objective function is (7) (this equation is called $f_1(p_i)$ for optimization) which shows the relationship used for generating MSDs. This equation must be minimized to reduce conflicts. The second objective function is shown as follows:

$$f_2(p_i) = p_i * \left(v_f \exp\left[\frac{-1}{a}\left(\frac{p_i}{k_m}\right)^a\right]\right). \tag{9}$$

Equation (10) shows the relationship for generating MFDs. This equation must be maximized to reach the capacity. However, in this study, use a minimizing function, so we use $-f_2(p)$. Thus, the generic formula for the current study problem optimization is presented in the following equation:

$$\begin{aligned}&\text{minimize } F(p_i) = \sum_{i=0}^{i=n} \alpha.\left(a.p_i^2 + b.p_i\right) - \sum_{i=0}^{i=n} \beta.\left(p_i * \left(v_f \exp\left\lfloor \frac{-1}{a}\left(\frac{p_i}{k_m}\right)^a \right\rfloor\right)\right),\\ &\text{subject to: } \frac{1}{3}.P_{\text{critical}} < p_i < P_{\text{critical}},\end{aligned} \tag{10}$$

where P_{critical} is critical density associated with the flow, α and β are weights of objective functions. These weights can vary between 0 and 1 so that 0 shows the least importance and 1 shows the highest importance. These weights help decision makers to find their optimal points based on different strategies and the importance of each objective function. This optimization model includes a critical constraint to avoid choosing a zero-density value when safety is prioritized ($b = 0$), which would unrealistically eliminate conflicts by not allowing any vehicle presence. To ensure practicality and efficiency, the model operates within a density range from 33% to 100% of the critical density, avoiding both the impractical extremes of zero density and full jam density. This approach guarantees the model uses at least a third of the road capacity, balancing road usage efficiency and safety considerations.

This study uses a nondominated sorting genetic algorithm (NSGA-II) algorithm to find the optimal points. NSGA-II was developed by Deb et al. [64] which by using a Pareto dominance relationship, the rank of solutions is determined using a fast, nondominated sorting algorithm those with a higher rank survive and are selected to reproduce [65]. Pareto fronts are a set of optimal solutions in a space of objective functions in multiobjective optimization problems (MOOPs) that are not dominant over each other but are best compared to the rest of the solutions [66]. As a result of its robust elitist strategy, focus on nondominated solutions, quick running speed, and diversity preservation mechanism, NSGA-II is uniquely competitive [67]. To explain the NSGA-II procedure, some steps are needed. In the first step, assume the initial population called P_t with the size of N. In the second step, after evaluating objective function and performing crossover and mutation on P_t, a new population is created called Q_t [68]. In the third step, the population that consists of P_t and Q_t is called R_t, so the nondominated sorting is done on R_t. At each stage, it selects the nondominant members and places them on one front and removes them from the population, placing the rest of the population on the next front in the same way. These steps continue until the entire population is on different fronts $(F_1, F_2, F_3, \ldots.)$ and this process is based on the Pareto front concept that the Pareto front consists of compromises that are acceptable for all objectives [67, 68]. The fourth step is calculating the crowding distance for members that are nondominant with each other. Solutions with larger crowding distances are preferred in this approach, which is determined by the average distance between two solutions along each of the objectives [65, 68]. In the fifth step, a tournament is used to select the population members for the next generation based on their rank and crowding distance called P_{t+1} [67, 68]. Until the stopping criteria are met, the procedure continues. In this study population size, maximum generations are equal to 20 and 100, respectively. Figure 1 shows the procedure of NSGA-II.

4. Results

In this study, a grid network that includes nine intersections was used to determine the impact of AVs on MFDs and MSDs. Each link in the network is 400 meters and bidirectional. Two speed limits were assessed 50 km/h and 30 km/h. The multiobjective optimization was performed on the 50 km/h speed limit, and the 30 km/h speed limit was used to compare the impact of the speed limit on MFDs and MSDs in presence of AVs. All traffic lights had a 90-second cycle time with a 43 second green phase, a 43 second red phase, and a 4 second yellow phase. Four turning movements were allowed at each intersection: straight, left turn, right turn, and U-turn. The grid network was routed randomly using Randomtrip.py (SUMO's built-in tool). Randomtrip.py in SUMO benefits from the period option which gives in the opportunity to control the traffic value and determine the rate of vehicle insertion in the network. By using this option, this study first generates vehicles randomly until there is congestion in the network. After this time, the rate of period option was reduced to reduce the number of vehicle insertions smoothly to eliminate congestion. The network generated by random trips was more homogeneous and flexible when compared to a grid model with fixed routes [29]. The duration of simulations is 1200s, and the data have been aggregated based on 1 min time intervals. In order to avoid gridlock, this study does not allow density to exceed 70 vehicles per kilometer, and the aggregated data has been ignored in each simulation where density exceeds 70 vehicles per kilometer. In our study, we conducted traffic simulations across various scenarios; each scenario was repeated 20 times to ensure data reliability and account for variability, thereby enhancing the robustness of our findings. Figure 2 shows the grid network. This scenario was considered high traffic demand; low and medium traffic demand are also presented in Section 4.5. The maximum density of low and medium demand is 18 veh/km and 45 veh/km, respectively.

4.1. Impact of AVs on MFDs and MSDs. Table 2 shows the statistical analysis of Papageorgiou speed-density model [56]. Where v_f is free-flow speed, p_c is critical density, a is the model shape parameter, and R^2, the goodness of fit measure. For each penetration rate R^2 is more than 0.98, demonstrating that the model provides a strong estimate of the relationship between speed and density.

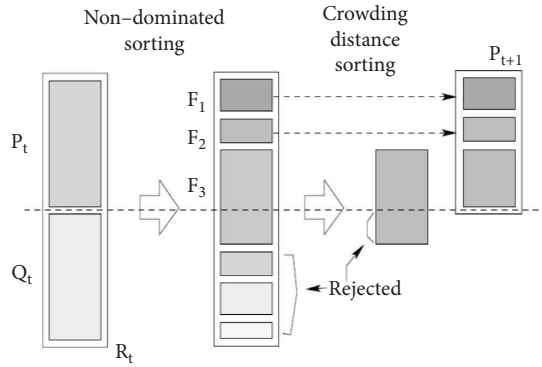

Figure 1: NSGA-II procedure [64].

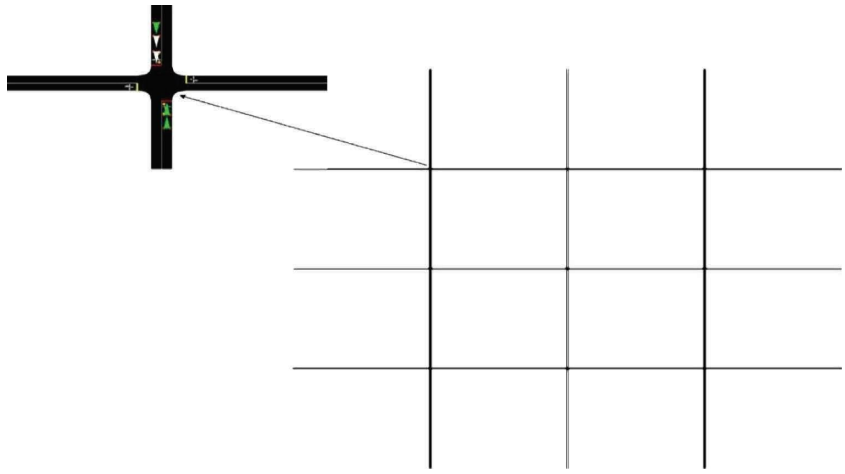

Figure 2: Case study grid network.

Table 2: Papageorgiou speed-density model [56] results.

MPR	V_f	P_c	A	R^2
0	47.11	30.02	0.89	0.99
20	46.66	32.13	0.88	0.99
40	43.73	31.32	0.99	0.98
60	44.09	36.07	0.93	0.98
80	43.02	41.98	0.98	0.98
100	43.34	49.14	0.93	0.98

The results presented in Table 3 shows that AVs increase critical density (P_c) by up to 63% when the MPR of AVs is 100%. Moreover, Figure 3 show the impact of AVs on average speed, capacity, and MFDs. The results confirm that AVs increase average speed and capacity by up to 21% and 59%, respectively. However, AVs have different effects depending on the penetration rate. When the MPR of AVs is 40%, the impact of AVs on MFDs is small with capacity, P_c, and average speed improving by 8%, 4%, and 6% respectively.

However, when MPR is 60%, AVs improve capacity, P_c and average speed 17%, 20%, and 13%, respectively, which shows that when AVs become the dominant flow, the effect of the AVs becomes more significant. In addition, when MPR is 100%, AVs increase capacity, P_c, and average speed 36%, 34%, and 7%, respectively, compared to when MPR is 60%.

To discuss the impact of AVs on MSDs, Table 4 shows the results of the statistical analysis of the MSDs model. R^2 values confirm that second-degree polynomial model can accurately estimate the relationship between conflicts and density. Table 4 includes information about the impact of AVs on CCP and CD. Table 3 shows that AVs can increase CD up to 31%. Also, Figure 4 illustrate that AVs reduced conflicts and CCP up to 80% and 75%, respectively. Thus, these changes confirm that AVs can improve the safety situation of urban networks substantially.

Table 3: Second-degree polynomial model results (MSD).

MPR	CCP	CD	R^2
0	207	38.39	0.87
20	216	39.11	0.88
40	195	40.14	0.87
60	185	42.96	0.92
80	126	48.25	0.88
100	52	50.37	0.80

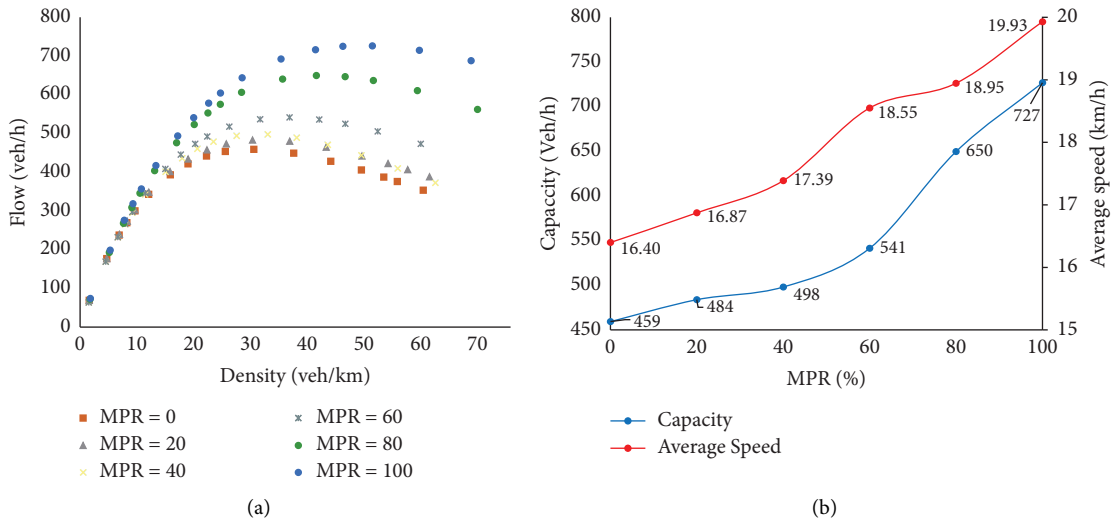

Figure 3: Impact of AVs on capacity, MFD, and average speed (speed limit = 50 km/h). (a) Flow-density diagram. (b) Change of capacity and average speed.

Table 4: Results of new capacity and CCP.

New capacity	New CCP	Capacity	Conflicts at capacity point	CCP	Capacity reduction	Conflicts at capacity point reduction	CCP reduction
409	145	459	197	207	10.94	26.33	29.98
428	153	484	209	216	11.55	26.76	29.08
445	141	498	187	195	10.65	24.68	27.86
477	140	541	183	185	11.90	23.46	24.30
577	96	650	125	126	11.19	23.08	24.05
645	41	727	52	52	11.25	21.15	21.15

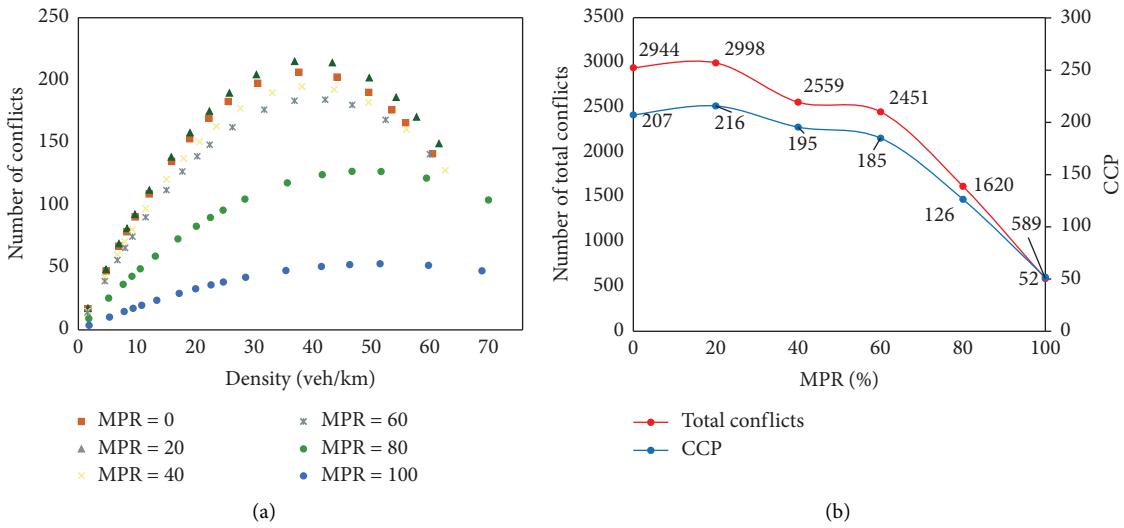

Figure 4: Impact of AVs on CCP, MSD, and total conflicts. (a) MSD. (b) Impact of CAVs on CCP and total conflicts.

It can be seen that AVs can improve MFDs and MSDs when AVs are dominant flow. However, at low penetration rates AVs are not expected to have a significant impact on MFDs and MSDs and that significant benefits are only achieved once penetration rates exceed 40%.

4.2. Time-Space Trajectory of HDVs and AVs. Based on disaggregated analysis, Figure 5 show trajectories (time-space) of each penetration rate. These trajectories show the whole network trajectories in a specific time period. Figure 5 shows when the penetration rate of AVs is increased the traffic jams are reduced substantially. Figure 5(a) shows the trajectory when MPR is equal to zero and all the vehicles are HDVs it can be realized that the stop-and-go waves are propagated backward from the intersection as a result of abrupt accelerations and decelerations. Stop-and-go waves reduce the passing speed of vehicles at intersections, thus decreasing the traffic throughput and increasing the chances of a collision [69]. Figures 5(b)–5(f) illustrate that when the penetration rate of AVs increases the stop-and-go waves decrease substantially. Thus, it can be concluded that AVs have the potential to increase flow and speed and decrease traffic jams. These figures confirm macroscopic results based on MFDs and MSDs results.

4.3. The Resulting Trade-Off between Capacity and Risk via the Multiobjective Optimization. In this section, the results of multi-objective optimization based on NSGA-II are presented. For this study, α and β are equal to 1. The value of α and β show the importance of each objective function in (10) and they can be changed based on the decision-makers traffic management strategy. Figure 6 shows the Pareto front solution using NSGA-II for different MPRs. These points are nondominance points among all possible solutions which are equal to the population size for each MPR. In addition to the values of α and β, Pareto front points represent alternative optimal points that decision-makers could choose based on their desired road network management strategy. Thus, this optimization method gives the decision-makers the opportunity to obtain their desired results based on different strategies in two ways. First, decision-makers can change the values of α and β based on the importance of each objective function. Second, decision-makers can choose their desired point from Pareto front points based on the different traffic management strategies.

To explain the importance of these points, assume a scenario. In this scenario, the values of α and β are set to 1, and we aim to select one point from each MPR to investigate to what extent these points can help to find a point in which not only the flow is high but also the number of conflicts is low. Thus, the main strategy is maintaining high flow and reducing conflicts. Table 4 shows the points that we selected from Pareto front points based on the above-mentioned main strategy. Generally, these points (new capacity and new CCP in Table 4) show that by reducing the traffic capacity by 10 to 12 percent, the number of maximum conflicts at the capacity point can be reduced from 21 to 27 percent, and in the case of CCDs from 21 to 30 percent. The points are a good indication of the main strategy that the selected points are the points where the flow is high, and the number of conflicts is low compared to the maximum number of conflicts. It is worth noting that the use of these points and values of α and β varies according to different strategies, and the flow can be reduced more than the stated amount to further reduce crashes. Moreover, it should be noted that these optimal points can be changed based on other strategies. For example, these findings seek to find points that are in the range of 8 to 12 percent reduction in flow, and subsequently seek the effect of this reduction in flow in reducing conflicts.

4.4. Impact of AVs in Low-Speed Limit Environments. In this section, the impact of AVs on MFDs and MSDs is presented. In Section 4.1, the speed limit was set to 50 km/h. In this section, the speed limit is 30 km/h. Using the Papageorgiou speed-density model [56] and second-degree polynomial model, MFDs and MSDs are generated. The statistical results of the two models confirm that the two models can accurately generate MSDs and MFDs. Appendix A presents the statistical results of the two models in detail. Figure 7 shows the impact of AVs on MFDs, capacity, and average speed. The impact of AVs on capacity is steadily increasing at each MPR, so that at each penetration percentage greater than 20%, the capacity increases by approximately 10%. The average speed results show that when the MPR is less than 60%, AVs do not have much effect on the average speed, but when the MPR reaches 60% and above, the average speed increases more dramatically. Figure 8 also shows the effect of AVs on MSDs, CCP, and total conflicts. This figure shows that when the MPR is less than 40%, the total number of conflicts and the CCP change very slightly. But when the MPR moves to 60% and above, the impact of AVs on the total number of conflicts and CCP increases. In general, the results show that for a dramatic change in the CCP, the average speed and the number of conflicts need to be dominated by AVs, but AVs increase capacity more continuously and significantly in low MPRs than the CCP. Moreover, Figure 9 shows the trajectory for each penetration rate. Like the 50 km/h scenarios, in the 30 km/h scenario, AVs have the ability to reduce stop-and-go waves and they can increase capacity and speed and decrease congestion and collisions. These results are in line with macroscopic results based on MFDs and MSDs results.

4.5. Impact of Speed Limits on AVs Effect on MFDs and MSDs. To compare the impact of speed limits on capacity, CCP, and total conflicts Figures 3, 5, and 10 must be compared. These figures can be interpreted in two ways. First, a comparison is made between speed limits when there are only HDVs in the network. In this condition, the capacity in the 50 km/h speed limit condition is 10% higher than the 30 km/h speed limit condition, while the total conflicts and CCP when the speed limit is 50 km/h are 15% and 18% higher than the 30 km/h speed limit condition. Thus, choosing the best speed limit varies based on the importance of safety or flow. Second, a comparison is made between speed limits when there are

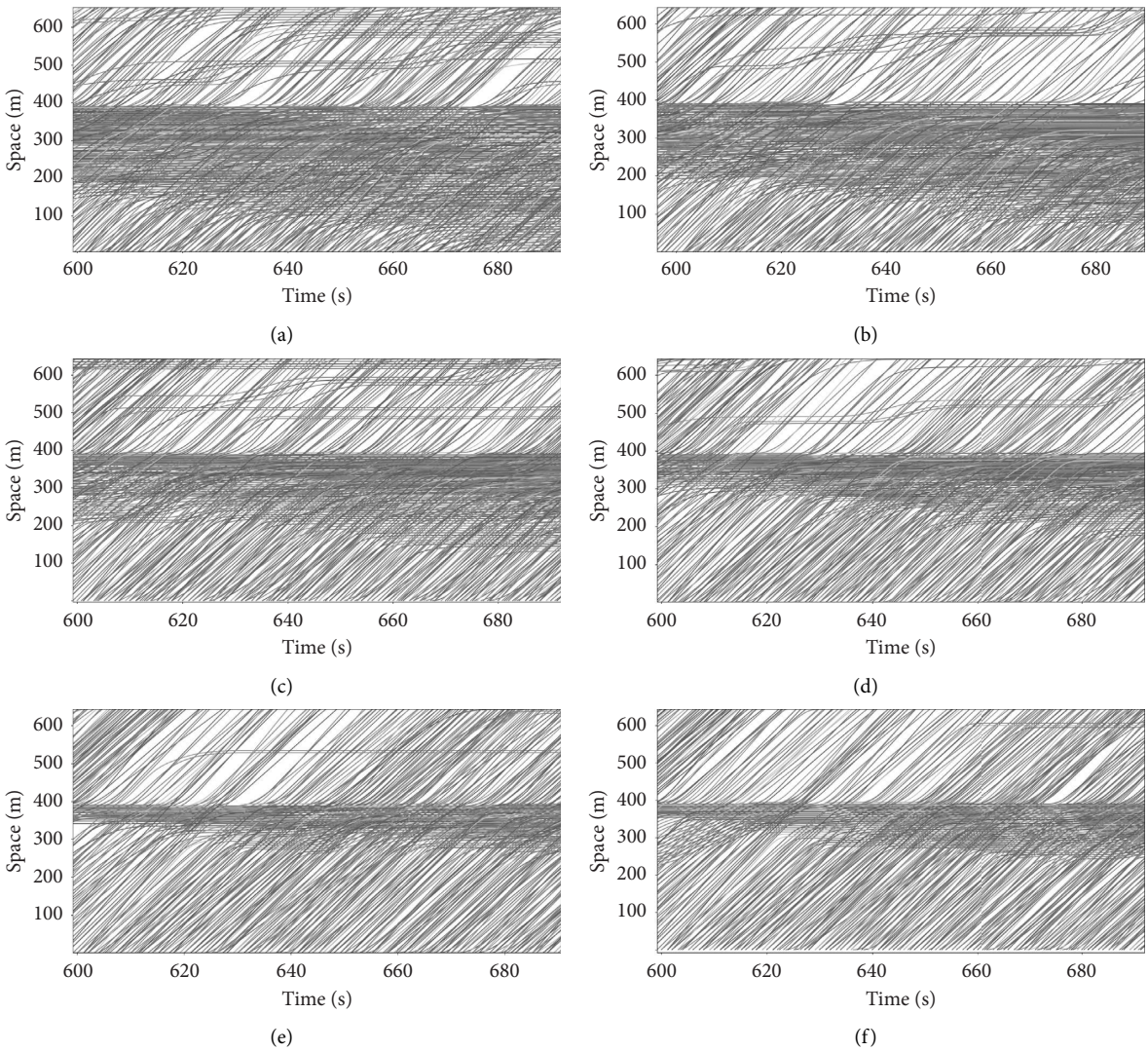

Figure 5: Vehicle trajectories along the grid network (speed limit = 50 km/h). (a) MPR = 0%. (b) MPR = 20%. (c) MPR = 40%. (d) MPR = 60%. (e) MPR = 80%. (f) MPR = 100%.

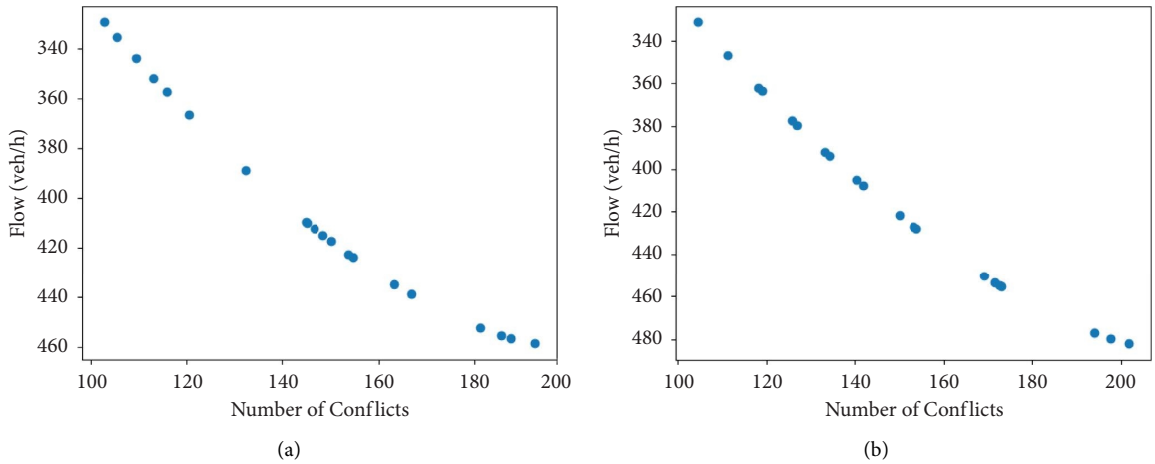

Figure 6: Continued.

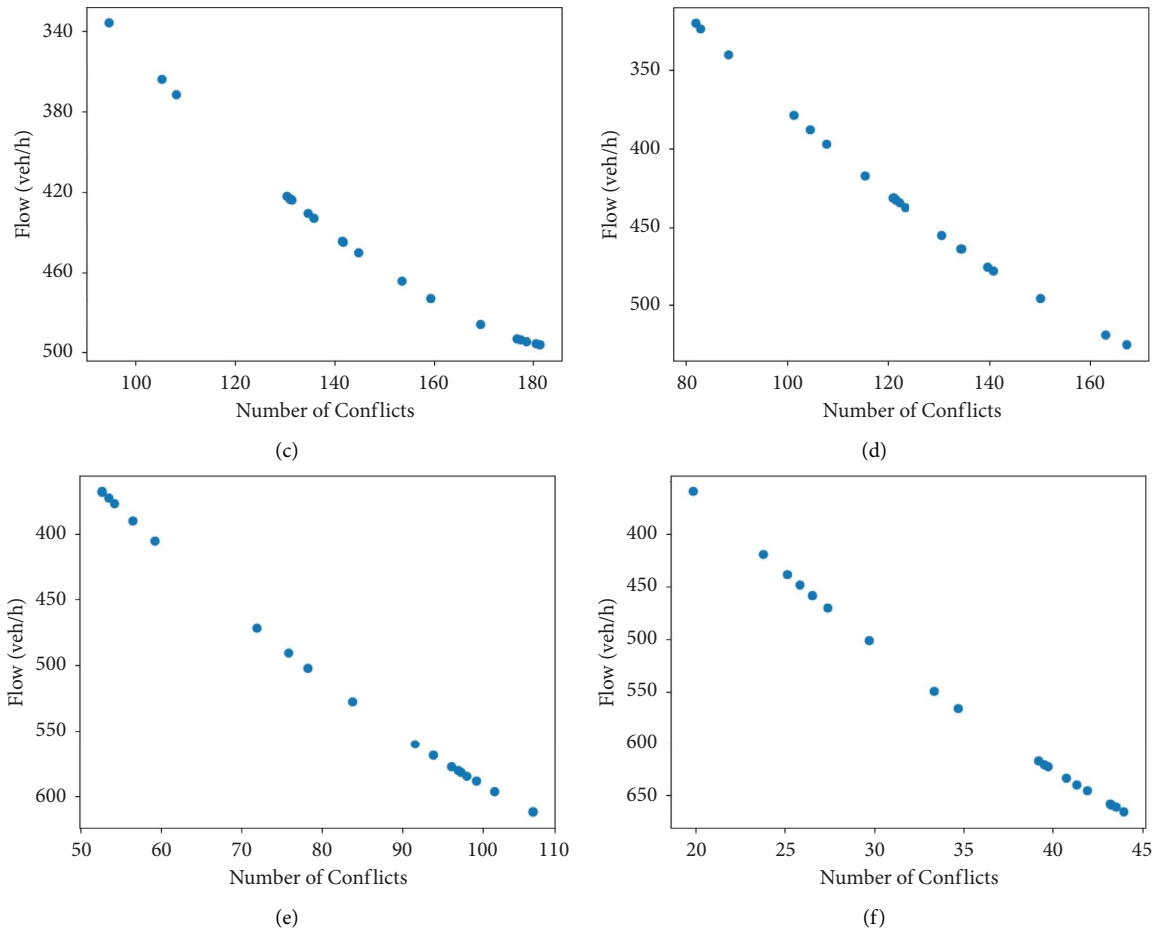

Figure 6: Pareto front solutions using NSGA-II for different MPRs. (a) MPR = 0%. (b) MPR = 20%. (c) MPR = 40%. (d) MPR = 60%. (e) MPR = 80%. (f) MPR = 100%.

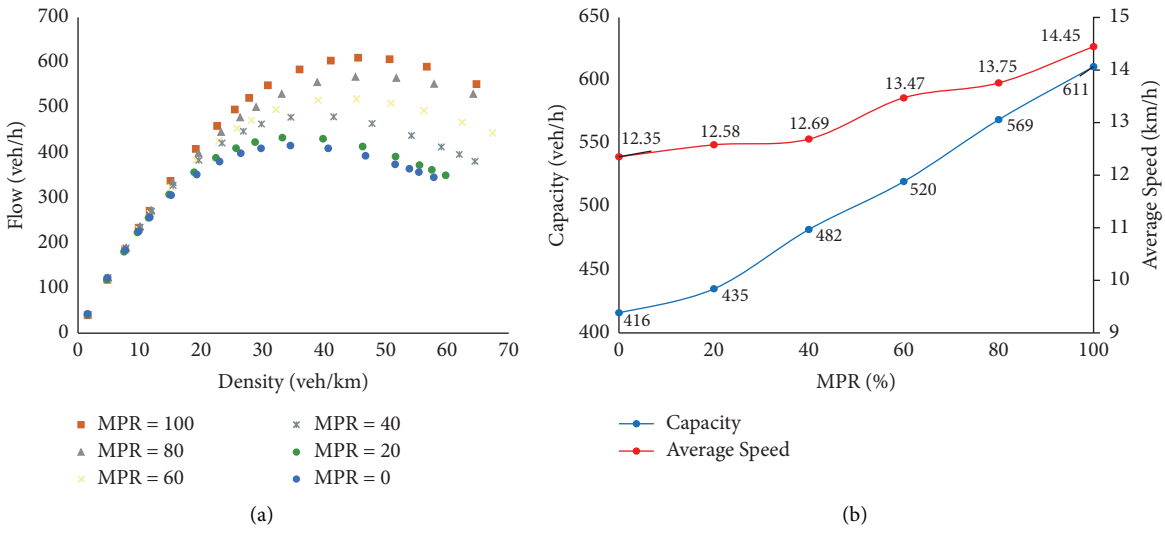

Figure 7: Impact of AVs on MFD, capacity, and average speed. (a) Flow-density diagram. (b) Change of capacity and average speed.

AVs in network. When the speed limit is 50 km/h, AVs increase capacity and average speed up to 59% and 21%, while at speed limits of 30 km/h, AVs increase capacity and average speed up to 46% by 17%. In addition, when the speed limit is 50 km/h, AVs reduce the total number of conflicts and AVs up to 80% and 75%, while when the speed limit is

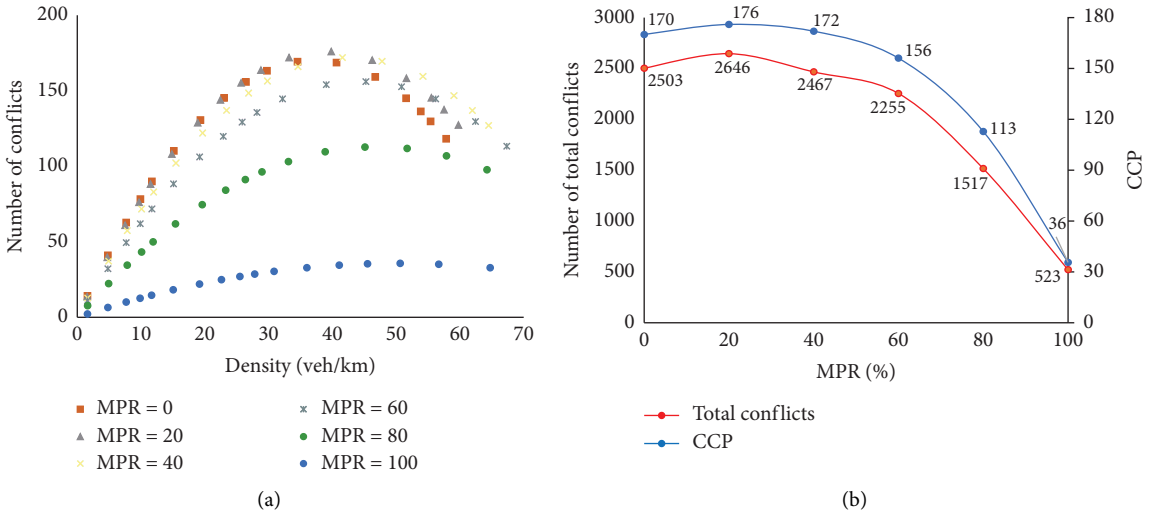

Figure 8: Impact of AVs on CCP, total conflicts and MSDs (speed limit = 30 km/h). (a) MSD. (b) Impact of CAVs on CCP and total conflicts.

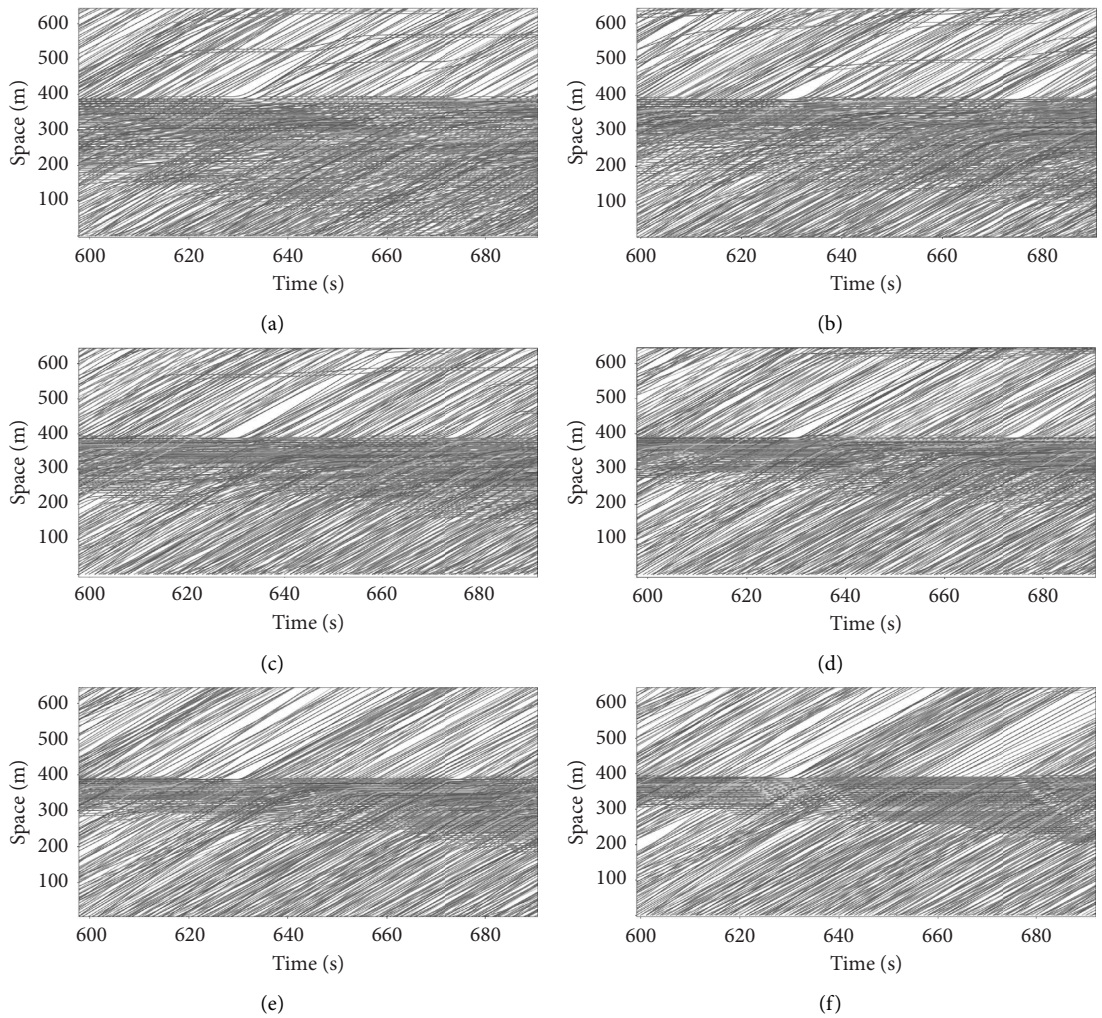

Figure 9: Vehicle trajectories along the grid network (speed limit = 30 km/h). (a) MPR = 0%. (b) MPR = 20%. (c) MPR = 40%. (d) MPR = 60%. (e) MPR = 80%. (f) MPR = 100%.

30 km/h, AVs reduce the total number of conflicts and CCP up to 80% and 79%. Generally, it can be realized that the impact of AV on capacity and average speed is more prominent in 50 km/h speed limit than in the 30 km/h speed limit, and AV's effect on safety is similar for both speed limits.

To compare the impact of AVs on MSDs and MFDs under different speed limits in detail, Figure 10 shows the impact of AVs on average speed, capacity, CCP, and total conflicts. Figure 10(a) confirms that AVs have a positive impact on CCP under the 50 km/h speed limit and 30 km/h speed limit. Based on the two-way ANOVA, the results show that there is no significant difference between the impact of AVs on CCP under two speed limits ($p = 0.31$). The 50 km/h speed limit condition did not meet the normality assumption of AVONA. Thus, the Kruskal–Wallis test, which is the nonparametric equivalent to the ANOVA, has been performed on the CCP change percentages for the two speed limits (50 km/h and 30 km/h). The test yielded a p value of approximately 0.810 which confirms that there is no significant difference between the impact of AVs on CCP under two speed limits.

Figure 10(b) illustrates when MPR is under 80%, the impact of AVs on capacity under 30 km/h is more than 50 km/h speed limit situation but when MPR is between 80% and 100%, the impact of AVs on capacity under 50 km/h speed limit is more than 30 km/h speed limit, so that when MPR is 100, the impact of AVs under 50 km/h speed limit is 24% more than when the speed limit is 30 km/h. Nevertheless, based on Table 5, the ANOVA analysis result shows that there is no statistically significant difference between the impact of AVs on capacity in the 50 km/h speed limit scenario compared to the 30 km/h speed limit ($p = 0.86$). Figure 10(c) shows that AVs have more impact on average speed under the 50 km/h speed limit. However, although Table 5 results show that the impact of AVs on average speed is significant ($p = 0.01$), it seems it is not sensible to compare the average speed under the different speed limits because it is obvious that the average speed under the 50 km/h speed limit is more than the average speed under the 30 km/h speed limit. Figure 10(d) confirms that AVs under the 50 km/h speed limit have a more positive impact on total conflict reduction in each MPR compared to the 30 km/h speed limit. Table 6 results for total conflicts show there is a statistically significant difference between the impact of AVs on total conflicts under the 50 km/h and 30 km/h speed limits ($p = 0.03$). Figure 10(e) illustrates that the impact of AVs on CD in a 30 km/h environment is more significant than in a 30 km/h environment when MPR is under 80, but because p value is 0.23 differences between the two speed limits' results are not significant. Figure 10(f) shows that in some MPRs, the impact of AVs on P_c in 30 km/h is more significant than 50 km/h environment, and vice versa. Although, based on Table 5 results, differences between the two speed limits' results are not significant ($p = 0.13$). It is worth mentioning that Table 5 confirms that the impact of all MPRs based on all metrics on two speed limits is significant.

4.6. The Impact of Different Levels of Congestion on Traffic Flow and Safety. This section explores the effect of AVs on traffic flow and safety under different levels of congestion. This study applied three different demand levels including low, medium, and high traffic demand. In low demand, the traffic situation is at an uncongested level which means that the network is far from reaching capacity. In medium traffic demand, the network reaches its capacity, but it is not highly congested. In high traffic demand, the network is highly congested, and there is gridlock on some links in the network. The previous sections' results were based on the high traffic demand. Generating different levels of demand in the network is applied using Randomtrip.py in the SUMO simulator. This build tool gives you this opportunity to define different levels of demand based on tunning a parameter called period.

To evaluate the traffic flow and the safety impact of AVs at different levels, the total number of conflicts, average speed, maximum flow, and maximum number of conflicts per time interval are used. The reason that capacity and CCP are not used is that in the low traffic demand, the network cannot reach capacity and CCP. Figures 11 and 12 show the results of different levels of congestion for the 50 km/h and 30 km/h speed limits. The maximum traffic flow results for both speed limits illustrate that with an increase in MPR and an increase in demand, the maximum flow increases. Also, the results show that as MPR increases, the difference between the maximum and average demand flow increases. Based on total conflicts and maximum conflicts results for two speed limits, as the MPR increases and demand decreases, the number of total conflicts and maximum conflicts reduces. However, the important point is that in contrast to the high congestion level when MPR is low, the number of total conflicts and maximum conflicts decreases which means that in low- and medium-demand situations, AVs can reduce conflicts even at lower rates of penetration. Moreover, the results of average speed based on two speed limits demonstrate that as the MPR increases, the average speed increases for all congestion levels but as demand increases, the average speed decreases. The reason is that when the demand increases from low to high, density increases, and consequently, the average speed decreases. Generally, the results show that AVs within the two speed limits and different congestion levels have the potential to improve traffic flow and decrease the risk of collision.

Tables 5 and 7 summarize the results of the two-way ANOVA of the impact of AVs on key traffic parameters for the two different speed limits at low and medium demand levels, respectively. The statistical data for high demand scenarios were addressed previously and are recorded in Table 6. This analysis for both demand levels shows that, similar to the findings for high demand, the MPR has a significant impact on all metrics assessed. In low-demand conditions, the influence of AVs on maximum flow and total conflicts does not show a statistically significant difference with two speed limits, while their impact on maximum conflicts and average speed does show a significant

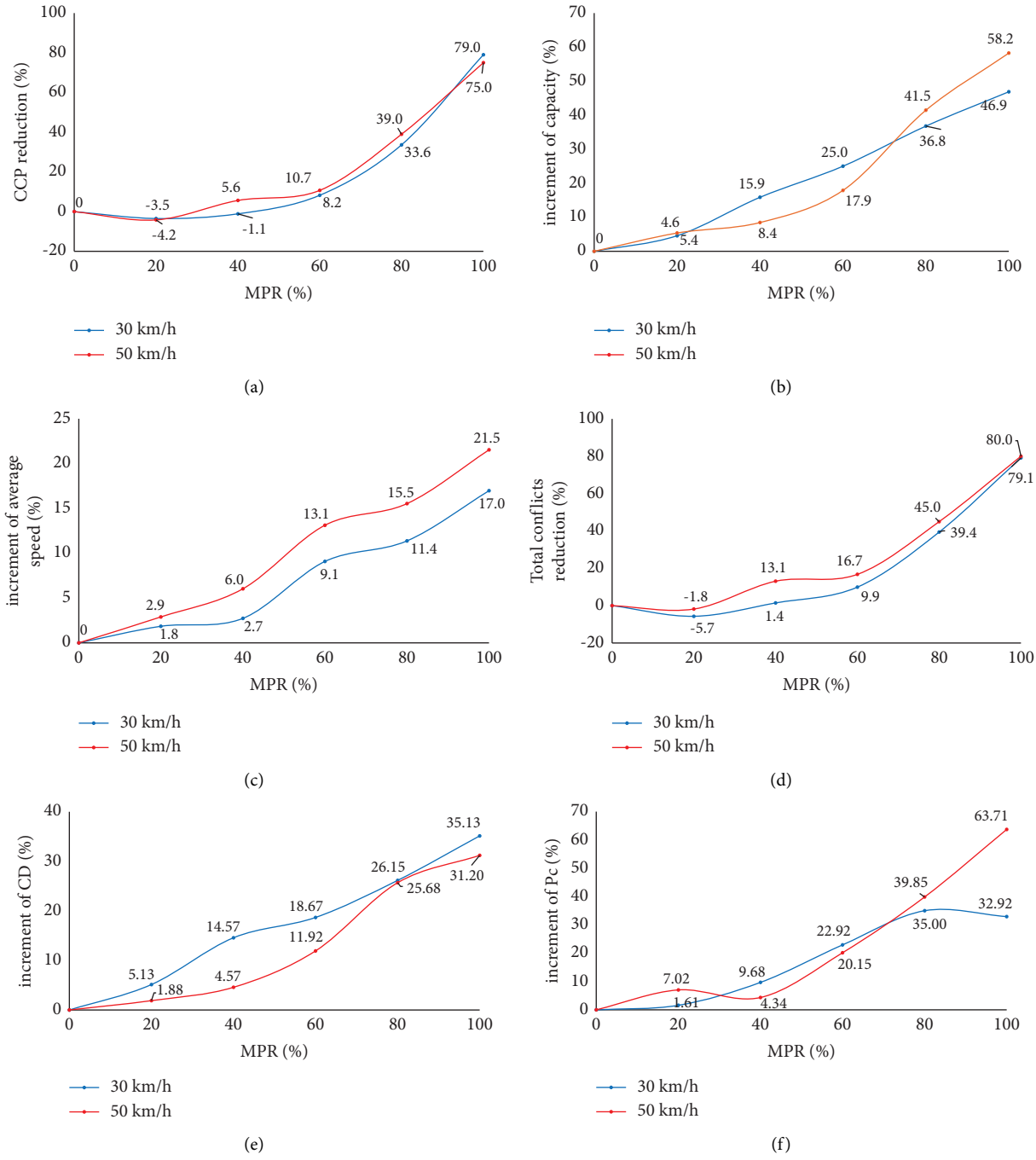

Figure 10: Comparison between impact of AVs on average speed, capacity, total conflicts, and CCP under two speed limits. (a) Impact of CAVs on CCP reduction. (b) Impact of CAVs on increment of capacity. (c) Impact of CAVs on increment of average speed. (d) Impact of CAVs on total conflicts reduction. (e) Impact of CAVs on increment of CD (%). (f) Impact of CAVs on increment of PC (%).

Table 5: Statistical analysis of impact of AVs on different metrics in two speed limits (low demand).

Metric	MPR		Speed limit		Normality (50 km/h)		Normality (30 km/h)		Homogeneity of variances	
	F value	*p* value	*F* value	*p* value	*F* value	*p* value	*F* value	*p* value	*F* value	*p* value
Total conflicts	160.9	<0.001	2.14	0.202	0.925	0.563	0.953	0.755	0.004	0.950
Maximum conflicts	693.8	<0.001	8.99	0.030	0.949	0.733	0.971	0.885	0.001	0.972
Average speed	13.1	0.006	19.58	0.006	0.915	0.467	0.942	0.675	1.171	0.304
Maximum flow	12.1	0.008	3.18	0.134	0.846	0.146	0.91	0.434	0.442	0.521

Table 6: Statistical analysis of impact of AVs on different metrics in two speed limits.

Metric	MPR		Speed limit		Normality (50 km/h)		Normality (30 km/h)		Homogeneity of variances	
	F value	*p* value	*F* value	*p* value	*F* value	*p* value	*F* value	*p* value	*F* value	*p* value
Total conflicts	227.19	<0.001	7.63	0.0397	0.864	0.2018	0.819	0.0864	0.0006	0.9806
CCP	248.6	<0.001	1.24	0.3160	0.778	0.0365	0.835	0.1192	0.0003	0.9871
Average speed	61.56	<0.001	13.64	0.0141	0.956	0.7902	0.924	0.5375	0.596	0.4579
Capacity	31.19	<0.001	0.03	0.8657	0.883	0.2813	0.957	0.7988	0.126	0.7302
CD	26.46	0.0013	1.81	0.2366	0.966	0.8637	0.882	0.2767	0.133	0.7229
P_c	12.12	0.008	3.18	0.1348	0.846	0.1463	0.91	0.4339	0.442	0.5211

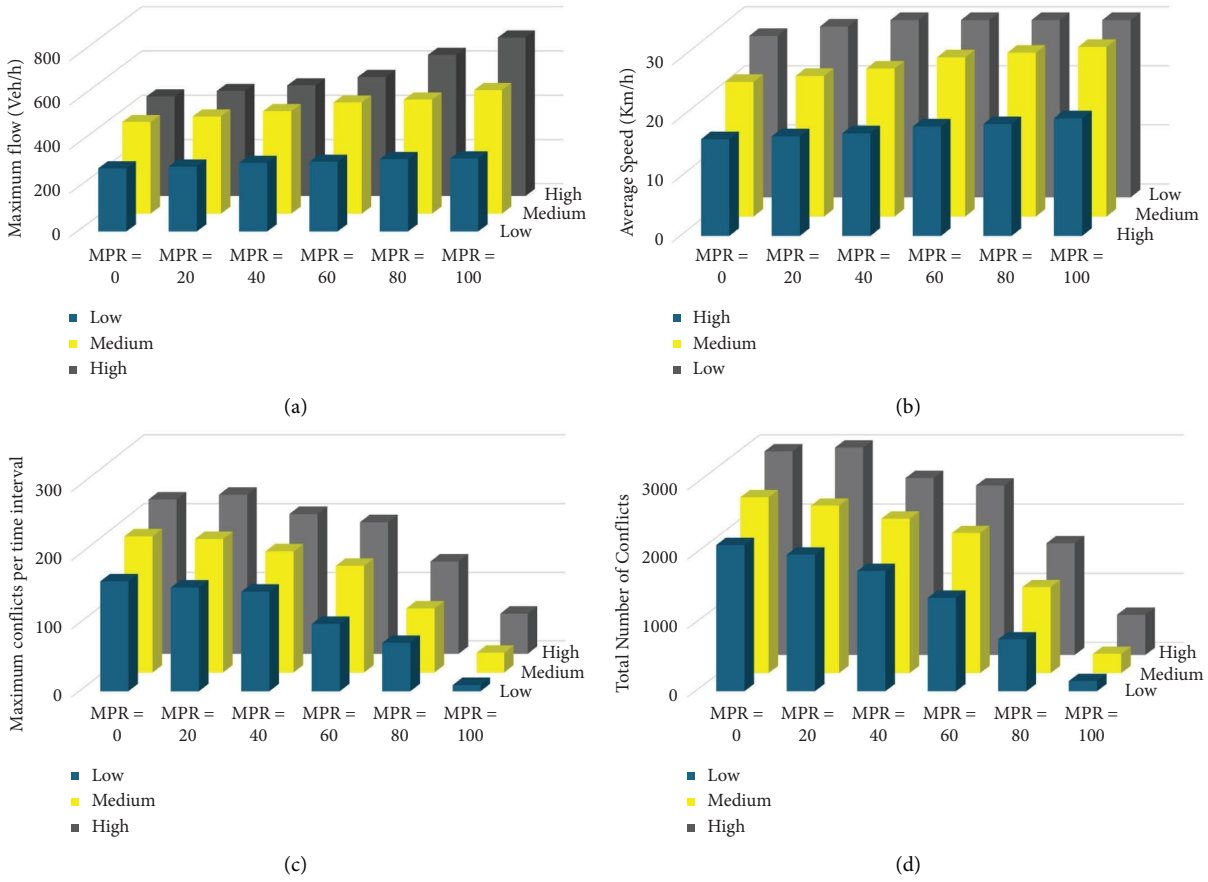

Figure 11: Traffic flow and safety results (speed limit = 50 km/h). (a) Traffic flow. (b) Average speed. (c) Maximum conflicts. (d) Total number of conflicts.

difference with two speed limits. In contrast, for medium demand, the effect of AVs on maximum flow shows a significant difference for both speed limits, but their impact on other metrics does not reveal a significant difference with two speed limits.

5. Discussions

This study investigated the impact of AVs on MFDs and MSDs, and more specifically, it investigated the network-level capacity, average speed, critical density, critical conflict point, critical density associated with maximum conflicts, and crash risk as a result of different levels of AV integration and operation.

This study has some key features which distinguish it from other studies. First, there are many studies that have investigated the impact of AVs on capacity and MFDs [10, 11, 22, 24, 25] or safety [16, 20, 21, 26, 29]. However, none of these studies have explored the impact of AVs on MFDs and MSDs simultaneously, and there is no study that has examined the impact of AVs on MSDs. The results of this study show that AVs can improve capacity, critical density,

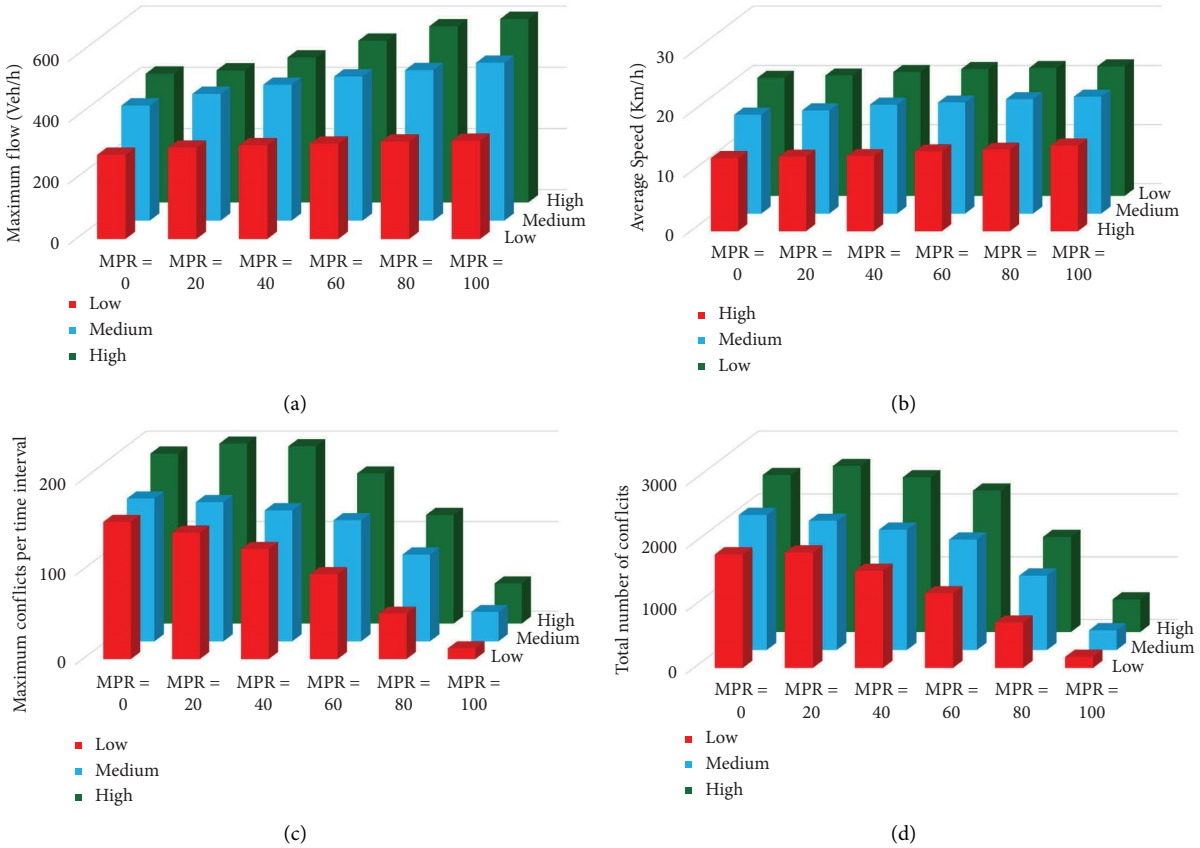

Figure 12: Traffic flow and safety results (speed limit = 30 km/h). (a) Traffic flow. (b) Average speed. (c) Maximum conflicts. (d) Total number of conflicts.

Table 7: Statistical analysis of impact of AVs on different metrics in two speed limits (medium demand).

Metric	MPR		Speed limit		Normality (50 km/h)		Normality (30 km/h)		Homogeneity of variances	
	F value	*p* value	*F* value	*p* value	*F* value	*p* value	*F* value	*p* value	*F* value	*p* value
Total conflicts	146.49	<0.001	4.9439	0.076	0.913	0.488	0.863	0.243	0.079	0.784
Maximum conflicts	876.53	<0.001	5.76	0.061	0.885	0.335	0.873	0.281	0.012	0.914
Average speed	21.56	0.002	4.69	0.082	0.957	0.790	0.977	0.918	2.03	0.184
Maximum flow	116.94	<0.001	15.67	0.010	0.979	0.930	0.988	0.971	0.017	0.899

and average speed which is in line with previous studies [10, 11, 22, 24, 25]. Also, the results show that AVs can reduce conflicts substantially which is in line with previous studies [16, 20, 21, 23], and AVs can reduce CCP and CD significantly. The important result is to quantify the network-level impact of the AVs, measured with the MFDs and MSDs, under variations in market penetration rate. When AVs dominate the flow, the impact of AVs on MFDs and MSDs is substantial compared to when HDVs are the dominant flow. This is a positive confirmation that the longer-term benefit of AVs to traffic operation can be substantial for the road network, though in the short term only marginal effects in crash reductions or network capacity improvements are expected (due to low presence). For urban road networks with typical grid structures such as the one used in this study, the lower-level threshold of market penetration for notable improvement is found to be 40%. The notable improvement of a penetration rate higher than 40% is primarily due to the fact that when penetration rates are high, the interaction between AVs and HDVs is low, and the dominant flow is AVs. Therefore, improvement in a higher penetration rate is made more significant. Some studies have shown that the percentage of automated vehicles will be at least 30% by 2040 and 100% after 2050 [70–73]. Thus, reducing congestion and improving safety with AVs is not a farfetched policy but a feasible policy and achieving 40% of this penetration rate can be achieved within the next few decades, so we can hope for a reduction in congestion and safety problems with AVs. It is worth mentioning that logically, there should be an upper-level threshold exceeding which the magnitude of operation improvement becomes marginal. The results of space-time

Table 8: Papageorgiou speed-density model [54] statistical analysis results (50 km/h).

MPR	Value			Standard error			T value			p value			R^2
	V_f	P_c	a	V_f	P_c	a	V_f	P_c	a	V_f	P_c	a	
0	47.11	30.02	0.89	1.7	1.2	0.05	27.43	24.85	16.92	$6.E-18$	$4.E-17$	$1.E-13$	0.99
20	46.66	32.13	0.88	1.8	1.4	0.06	24.95	21.64	15.06	$4.E-17$	$7.E-16$	$9.E-13$	0.99
40	43.73	31.32	0.99	1.6	1.3	0.07	26.76	22.60	14.54	$1.E-17$	$3.E-16$	$1.E-12$	0.98
60	44.09	36.07	0.93	1.5	1.7	0.06	27.98	21.00	15.12	$4.E-18$	$1.E-15$	$9.E-13$	0.98
80	43.02	41.98	0.98	1.5	2.0	0.07	27.44	20.32	14.15	$6.E-18$	$2.E-15$	$3.E-12$	0.98
100	43.34	49.14	0.93	1.66	2.85	0.07	26.24	17.23	13.39	$1E-17$	$7.E-14$	$9.E-12$	0.98

Table 9: Second-degree polynomial model statistical analysis results (MSD).

MPR	Value		Standard error		T value		p value		R^2
	a	b	a	b	a	b	a	b	
0	−0.141	10.78	0.009	0.575	−14.961	18.772	0.00	$5.17E-13$	0.87
20	−0.141	11.03	0.009	0.581	−15.114	18.994	$3.91E-15$	$4.22E-13$	0.88
40	−0.128	9.98	0.009	0.573	−14.305	17.424	$2.33E-14$	$1.27E-12$	0.87
60	−0.116	9.25	0.006	0.411	−18.249	22.497	$1.12E-16$	$8.96E-15$	0.92
80	−0.054	5.24	0.004	0.299	−14.313	17.502	$1.26E-12$	$2.12E-14$	0.88
100	−0.020	2.05	0.003	0.239	−7.371	8.620	$2.24E-07$	$1.67E-08$	0.80

Table 10: Papageorgiou speed-density model [54] statistical analysis results (30 km/h).

MPR	Value			Standard error			T value			p value			R^2
	V_f	P_c	a	V_f	P_c	a	V_f	P_c	a	V_f	P_c	a	
0	27.67	34.97	1.18	$1E-14$	$2E-14$	$1E-15$	$1E+14$	$1E+15$	$6E+14$	0	0	0	0.99
20	26.87	35.53	1.27	0.78	1.10	0.09	34.52	32.21	14.28	$5E-20$	$2E-19$	$2E-12$	0.98
40	26.32	38.35	1.35	0.80	1.24	0.10	32.95	30.94	13.08	$1E-19$	$5E-19$	$1E-11$	0.98
60	26.30	42.98	1.29	0.76	1.53	0.10	34.65	28.06	13.47	$5E-20$	$3E-18$	$8E-12$	0.98
80	26.14	47.20	1.29	0.79	1.86	0.10	33.07	25.34	12.65	$1E-19$	$3E-17$	$2E-11$	0.98
100	25.19	46.48	1.54	0.67	1.56	0.12	37.68	29.89	12.98	$9E-21$	$1E-18$	$1E-11$	0.98

Table 11: Second-degree polynomial model statistical analysis results.

MPR	Value		Standard error		T value		p value		R^2	CD
	a	b	a	b	a	b	a	b		
0	−0.123	9.133	0.007	0.422	−16.964	21.631	$2.5E-16$	$4.0E-14$	0.87	37.25
20	−0.115	8.991	0.010	0.601	−11.370	14.955	$1.1E-10$	$5.2E-13$	0.87	39.16
40	−0.094	8.062	0.006	0.411	−15.443	19.600	$2.7E-13$	$2.0E-15$	0.9	42.67
60	−0.080	7.065	0.005	0.350	−16.065	20.165	$1.2E-13$	$1.1E-15$	0.9	44.20
80	−0.051	4.806	0.002	0.197	−20.519	24.426	$7.7E-16$	$1.9E-17$	0.93	46.98
100	−0.014	1.418	0.002	0.180	−6.412	7.868	$1.8E-06$	$7.7E-08$	0.79	50.33

diagrams also confirm that AVs can reduce stop-and-go waves, and as a consequence, AVs can increase critical density and capacity, and they can improve safety. Generally, microscopic results confirm macroscopic results.

The results show that AVs have the potential to increase the average speed across the network. Even when the mode share of the AVs is not high and distributed sparsely, there is still the benefit of "moving more efficiently" for the entire network. While it is promising to see that increasing speed is coupled with reducing conflicts, higher speeds of vehicles are associated with increased crash risk and severity, particularly for other modes of transportation, especially vulnerable road users [74–76]. In cases of more than moderate increase in average speed (for example, "moderate increase" can be some percentage over an average speed limit that is estimated from the MSD), warnings should be given to the driving assistant or control systems so that the systems can activate the emergency responses in various scenarios proactively.

The MSDs show that until the capacity and the critical density are reached, there is no common benefit between flow (i.e., network efficiency) and conflicts (i.e., network safety). The applied multiobjective optimization is demonstrated to be useful to identify some suboptimal sets of operation points. For example, on average, these suboptimal operation solutions see a drop in capacity of 10 to 12 percent,

while they see a more drastic reduction in the number of maximum conflicts from 21 to 27 percent and in CCDs from 21 to 30 percent. While the numbers are network-specific, such operation concepts are rarely discussed in literature, and they provide alternatives and mobility targets for the operators. Potentially, another dimension that could be incorporated into the analysis is variable speed limits and even dedicated lane allocations to further increase the benefit of having AVs in the system. This, however, requires more efficient algorithms to handle real-time implementation (the complexity of the optimization problem of a flow-safety-speed limit trade-off is extremely high).

With regard to speed limits, this study demonstrates the benefits of AVs operating in low-speed limit traffic environments. Our results indicate that the change in speed limit has a minor impact when the network has only HDVs (the number of conflicts and capacity has a 15% and 10% negative difference, as speed limit drops from 50 km/h to 30 km/h). However, when there are only AVs in the network, the operation improvement is significant compared to the HDV-only scenario, aligning with the research's findings on safety and efficiency carried out by Lu et al. [77]. Moreover, this study investigated the impact of AVs on traffic flow and safety based on different congestion levels. The results confirmed that at all congestion levels, AVs improved traffic flow, increased average speed, and demonstrated that AVs can improve safety, even at low MPRs.

The findings of this study show that the presence of AVs has the potential to reduce the dilemma between mobility efficiency and safety. Based on this study and literature, AVs, given their control features, offer the advantages of increasing average speed, reducing conflicts, and increasing capacity at a network-wide scale [10, 16, 20]. In addition, to balance the mobility goals, this research provided a multi-objective optimization-driven tool which can help users identify the optimal trade-offs between the objectives. This multiobjective optimization-driven tool allows city planners and network operators to develop dynamic strategies based on current infrastructure or traffic management priorities.

This study includes some limitations that future studies could seek to address. This study makes several assumptions regarding how AVs operate. For example, it assumes that AVs follow AVs and HDVs with the same driving behavior. As more information becomes available about AV technology, these behaviors can be more accurately simulated which could influence the findings.

An important element of this study was the demonstration of how AVs can influence MSDs and MDFs; however, the network used for analysis was simplistic. Furthermore, this study focuses on a grid network where each road has a single lane in each direction, which means the effects of AVs lane-changing behaviors are not examined in this research. Future studies are encouraged to explore grid networks with multiple lanes in each direction to better understand how AVs' lane-changing actions might impact traffic flow and safety. Beyond this, studies could consider real-world urban networks under different congestion levels, while broadening the optimization modeling by considering additional factors such as GHG emissions or air pollution to provide a more holistic view of the impacts of AVs.

Appendix

Tables 8 and 9 show the results of statistical analysis of the speed-density model and second-degree polynomial model. To show that based on simulation data, the Papageorgiou speed-density model [56] and the second-degree polynomial model can accurately show the relationship between speed-density and conflict-density, respectively, this study used R^2, T-values, and p values. R^2 values demonstrate the strength of the relationship between speed-density and conflict-density. All t-values that are far from zero and p values that are smaller than 0.05, as in this model, would indicate that the null hypothesis is rejected, and there are relationships between speed-density and conflict-density based on the Papageorgiou speed-density model [56] and second-degree polynomial model. v_f is free-flow speed, p_c is critical density, and a is the model shape parameter.

Tables 10 and 11 show the results of statistical analysis of the speed-density model and the second-degree polynomial model. Two model p values and T-values and R^2 values confirm that two models can accurately estimate the relationship between speed-density and conflicts-density.

Data Availability

Data available on request: Contact karbaa3@mcmaster.ca.

Additional Points

Highlights. Investigated the impact of AVs on road network operational characteristics. Analyzed the benefit of AV presence of increased capacity and reduced conflicts at a network-level. Conducted optimization-driven analysis on the tradeoff between efficiency and safety. Investigated how AVs affect average speed of urban networks and speed-safety conflict

Conflicts of Interest

The authors declare that they have no conflicts of interest.

Acknowledgments

KA is a PhD researcher at the McMaster University. NZ is a full time academic staff member at Monash University. SO is a full time academic staff member at the University of Leeds. Open Access funding enabled and organized by JISC.

References

[1] F. Ding, J. Jiang, Y. Zhou, R. Yi, and H. Tan, "Unravelling the impacts of parameters on surrogate safety measures for a mixed platoon," *Sustainability*, vol. 12, no. 23, p. 9955, 2020.

[2] P. Liu and W. D. Fan, "Exploring the impact of connected and autonomous vehicles on mobility and environment at signalized intersections through vehicle-to-infrastructure (V2I) and infrastructure-to-vehicle (I2V) communications," *Transportation Planning and Technology*, vol. 44, no. 2, pp. 129–138, 2021.

[3] M. Massar, I. Reza, S. M. Rahman, S. M. H. Abdullah, A. Jamal, and F. S. Al-Ismail, "Impacts of autonomous vehicles on greenhouse gas emissions—positive or negative?" *International Journal of Environmental Research and Public Health*, vol. 18, no. 11, p. 5567, 2021.

[4] T. Niels, M. Erciyas, and K. Bogenberger, "Impact of connected and autonomous vehicles on the capacity of signalized intersections–Microsimulation of an intersection in Munich," in *Proceedings of the 7th Transport Research Arena TRA 2018*, Vienna, Austria, March, 2018.

[5] Inrix, *Americans Lost 3.4 Billion Hours Due to Congestion in 2021, 42% below Pre-COVID*, 2021.

[6] National Center for Statistics and Analysis, "Early estimate of motor vehicle traffic fatalities for the first half (January–June) of 2021 rep. Crash•Stats brief statistical summary," Report No. DOT HS 813 199, National Highway Traffic Safety Administration, New Jersey, NJ, USA, 2021.

[7] P. Bansal and K. M. Kockelman, "Forecasting Americans' long-term adoption of connected and autonomous vehicle technologies," *Transportation Research Part A: Policy and Practice*, vol. 95, pp. 49–63, 2017.

[8] D. Lee and D. J. Hess, "Regulations for on-road testing of connected and automated vehicles: assessing the potential for global safety harmonization," *Transportation Research Part A: Policy and Practice*, vol. 136, pp. 85–98, 2020.

[9] B. Sheehan, F. Murphy, M. Mullins, and C. Ryan, "Connected and autonomous vehicles: a cyber-risk classification framework," *Transportation Research Part A: Policy and Practice*, vol. 124, pp. 523–536, 2019.

[10] L. Atkins, "Research on the impacts of connected and autonomous vehicles (AVs) on traffic flowRep," Department of Transport, 2016.

[11] P. Liu and W. Fan, "Exploring the impact of connected and autonomous vehicles on freeway capacity using a revised Intelligent Driver Model," *Transportation Planning and Technology*, vol. 43, no. 3, pp. 279–292, 2020.

[12] A. Haghi, D. Ketabi, M. Ghanbari, and H. Rajabi, "Assessment of human errors in driving accidents; analysis of the causes based on aberrant behaviors," *Life Science Journal*, vol. 11, no. 9, pp. 414–420, 2014.

[13] Who, "Road traffic injuries," 2021.

[14] A. Dixit, R. Kumar Chidambaram, and Z. Allam, "Safety and risk analysis of autonomous vehicles using computer vision and neural networks," *Vehicles*, vol. 3, no. 3, pp. 595–617, 2021.

[15] V. V. Dixit, S. Chand, and D. J. Nair, "Autonomous vehicles: disengagements, accidents and reaction times," *PLoS One*, vol. 11, no. 12, Article ID e0168054, 2016.

[16] A. Papadoulis, M. Quddus, and M. Imprialou, "Evaluating the safety impact of connected and autonomous vehicles on motorways," *Accident Analysis and Prevention*, vol. 124, pp. 12–22, 2019.

[17] A. Sinha, S. Chand, K. P. Wijayaratna, N. Virdi, and V. Dixit, "Comprehensive safety assessment in mixed fleets with connected and automated vehicles: a crash severity and rate evaluation of conventional vehicles," *Accident Analysis and Prevention*, vol. 142, Article ID 105567, 2020a.

[18] A. Sinha, S. Chand, K. P. Wijayaratna, N. Virdi, and V. Dixit, "Crash severity and rate evaluation of conventional vehicles in mixed fleets with connected and automated vehicles," *Procedia Computer Science*, vol. 170, pp. 688–695, 2020b.

[19] A. Sinha, V. Vu, S. Chand, K. Wijayaratna, and V. Dixit, "A crash injury model involving autonomous vehicle: investigating of crash and disengagement reports," *Sustainability*, vol. 13, no. 14, p. 7938, 2021.

[20] N. Virdi, H. Grzybowska, S. T. Waller, and V. Dixit, "A safety assessment of mixed fleets with connected and autonomous vehicles using the surrogate safety assessment module," *Accident Analysis and Prevention*, vol. 131, pp. 95–111, 2019.

[21] R. Arvin, A. J. Khattak, M. Kamrani, and J. Rio-Torres, "Safety evaluation of connected and automated vehicles in mixed traffic with conventional vehicles at intersections," *Journal of Intelligent Transportation Systems*, vol. 25, no. 2, pp. 170–187, 2020.

[22] A. Ghiasi, O. Hussain, Z. S. Qian, and X. Li, "A mixed traffic capacity analysis and lane management model for connected automated vehicles: a Markov chain method," *Transportation Research Part B: Methodological*, vol. 106, pp. 266–292, 2017.

[23] A. Karbasi and S. O'Hern, "Investigating the impact of connected and automated vehicles on signalized and unsignalized intersections safety in mixed traffic," *Future Transportation*, vol. 2, no. 1, pp. 24–40, 2022.

[24] M. Martin-Gasulla, P. Sukennik, and J. Lohmiller, "Investigation of the impact on throughput of connected autonomous vehicles with headway based on the leading vehicle type," *Transportation Research Record*, vol. 2673, no. 5, pp. 617–626, 2019.

[25] J. A. Shelton, "Revolutionizing our roadways: modeling the traffic impacts from automated and connected vehicles in a complex, congested urban setting," *Texas A and M Transportation Institute*, 2016.

[26] H. Zhang, N. Hou, J. Zhang, X. Li, and Y. Huang, "Evaluating the safety impact of connected and autonomous vehicles with lane management on freeway crash hotspots using the surrogate safety assessment model," *Journal of Advanced Transportation*, vol. 2021, Article ID 5565343, 14 pages, 2021.

[27] A. Talebpour and H. S. Mahmassani, "Influence of connected and autonomous vehicles on traffic flow stability and throughput," *Transportation Research Part C: Emerging Technologies*, vol. 71, pp. 143–163, 2016.

[28] L. Xiao, M. Wang, W. Schakel, and B. van Arem, "Unravelling effects of cooperative adaptive cruise control deactivation on traffic flow characteristics at merging bottlenecks," *Transportation Research Part C: Emerging Technologies*, vol. 96, pp. 380–397, 2018.

[29] A. H. Karbasi, B. B. Mehrabani, M. Cools, L. Sgambi, and M. Saffarzadeh, "Comparison of speed-density models in the age of connected and automated vehicles," *Transportation Research Record*, vol. 2677, no. 3, pp. 849–865, 2023.

[30] R. Alsalhi, V. V. Dixit, and V. V. Gayah, "On the existence of network Macroscopic Safety Diagrams: theory, simulation and empirical evidence," *PLoS One*, vol. 13, no. 8, Article ID e0200541, 2018.

[31] M. T. Islam, "Investigating the speed and rear-end collision relationship at urban signalized intersections," *Transportation Research Record*, vol. 2601, no. 1, pp. 10–16, 2016.

[32] A. E. Retallack and B. Ostendorf, "Relationship between traffic volume and accident frequency at intersections," *International Journal of Environmental Research and Public Health*, vol. 17, no. 4, p. 1393, 2020.

[33] Z.-H. Jiang, X.-G. Yang, T. Sun, T. Wang, and Z. Yang, "Investigating the relationship between traffic violations and crashes at signalized intersections: an empirical study in China," *Journal of Advanced Transportation*, vol. 2021, Article ID 4317214, 8 pages, 2021.

[34] A. Ahmed, D. Ngoduy, M. Adnan, and M. A. U. Baig, "On the fundamental diagram and driving behavior modeling of

heterogeneous traffic flow using UAV-based data," *Transportation Research Part A: Policy and Practice*, vol. 148, pp. 100–115, 2021.
[35] J. Godfrey, "The mechanism of a road network," *Traffic Engineering and Control*, vol. 8, no. 8, 1969.
[36] H. Mahmassani, J. C. Williams, and R. Herman, "Performance of urban traffic networks," *Proceedings of the 10th International Symposium on Transportation and Traffic Theory*, Elsevier Science Publishing, pp. 1–20, Amsterdam, Netherlands, 1987.
[37] C. F. Daganzo, "Urban gridlock: macroscopic modeling and mitigation approaches," *Transportation Research Part B: Methodological*, vol. 41, no. 1, pp. 49–62, 2007a.
[38] N. Geroliminis and C. F. Daganzo, "Existence of urban-scale macroscopic fundamental diagrams: some experimental findings," *Transportation Research Part B: Methodological*, vol. 42, no. 9, pp. 759–770, 2008.
[39] N. Geroliminis and J. Sun, "Hysteresis phenomena of a macroscopic fundamental diagram in freeway networks," *Procedia-Social and Behavioral Sciences*, vol. 17, pp. 213–228, 2011.
[40] L. Bellocchi and N. Geroliminis, "Unraveling reaction-diffusion-like dynamics in urban congestion propagation: insights from a large-scale road network," *Scientific Reports*, vol. 10, no. 1, pp. 4876–4911, 2020.
[41] N. Geroliminis, N. Zheng, and K. Ampountolas, "A three-dimensional macroscopic fundamental diagram for mixed bi-modal urban networks," *Transportation Research Part C: Emerging Technologies*, vol. 42, pp. 168–181, 2014.
[42] C. Huang, N. Zheng, and J. Zhang, "Investigation of bimodal macroscopic fundamental diagrams in large-scale urban networks: empirical study with GPS data for Shenzhen city," *Transportation Research Record*, vol. 2673, no. 6, pp. 114–128, 2019.
[43] N. Zheng and N. Geroliminis, "Area-based equitable pricing strategies for multimodal urban networks with heterogeneous users," *Transportation Research Part A: Policy and Practice*, vol. 136, pp. 357–374, 2020.
[44] N. Zheng, G. Rérat, and N. Geroliminis, "Time-dependent area-based pricing for multimodal systems with heterogeneous users in an agent-based environment," *Transportation Research Part C: Emerging Technologies*, vol. 62, pp. 133–148, 2016.
[45] K. Ampountolas, N. Zheng, and N. Geroliminis, "Macroscopic modelling and robust control of bi-modal multi-region urban road networks," *Transportation Research Part B: Methodological*, vol. 104, pp. 616–637, 2017.
[46] K. Yang, N. Zheng, and M. Menendez, "Multi-scale perimeter control approach in a connected-vehicle environment," *Transportation Research Procedia*, vol. 23, pp. 101–120, 2017.
[47] T. Dantsuji, D. Fukuda, and N. Zheng, "Simulation-based joint optimization framework for congestion mitigation in multimodal urban network: a macroscopic approach," *Transportation*, vol. 48, no. 2, pp. 673–697, 2021.
[48] F. Zhang, N. Zheng, H. Yang, and N. Geroliminis, "A systematic analysis of multimodal transport systems with road space distribution and responsive bus service," *Transportation Research Part C: Emerging Technologies*, vol. 96, pp. 208–230, 2018.
[49] R. Wiedemann, "Simulation des strassenverkehrsflusses," Schriftenreihe des Instituts fr Verkehrswesen der Universitt Karlsruhe, Karlsruhe,Germany, 1974.
[50] S. C. Calvert, W. J. Schakel, and J. W. C. Van Lint, "Will automated vehicles negatively impact traffic flow?" *Journal of Advanced Transportation*, vol. 2017, Article ID 3082781, 17 pages, 2017.
[51] M. Montanino and V. Punzo, "On string stability of a mixed and heterogeneous traffic flow: a unifying modelling framework," *Transportation Research Part B: Methodological*, vol. 144, pp. 133–154, 2021.
[52] M. Shang and R. E. Stern, "Impacts of commercially available adaptive cruise control vehicles on highway stability and throughput," *Transportation Research Part C: Emerging Technologies*, vol. 122, Article ID 102897, 2021.
[53] H. Manivasakan, R. Kalra, S. O'Hern, Y. Fang, Y. Xi, and N. Zheng, "Infrastructure requirement for autonomous vehicle integration for future urban and suburban roads – Current practice and a case study of Melbourne, Australia," *Transportation Research Part A: Policy and Practice*, vol. 152, pp. 36–53, 2021.
[54] X. Zou, S. O'Hern, B. Ens et al., "On-road virtual reality autonomous vehicle (VRAV) simulator: An empirical study on user experience," *Transportation Research Part C: Emerging Technologies*, vol. 126, Article ID 103090, 2021.
[55] P. A. Lopez, M. Behrisch, L. Bieker-Walz et al., "Microscopic traffic simulation using SUMO," in *Proceedings of the 2018 21st International Conference on Intelligent-Transportation Systems (ITSC)*, pp. 2575–2582, Maui, HI, USA, November, 2018.
[56] M. Papageorgiou, J.-M. Blosseville, and H. Hadj-Salem, "Macroscopic modelling of traffic flow on the Boulevard Périphérique in Paris," *Transportation Research Part B: Methodological*, vol. 23, no. 1, pp. 29–47, 1989.
[57] U. Durrani, C. Lee, and H. Maoh, "Calibrating the Wiedemann's vehicle-following model using mixed vehicle-pair interactions," *Transportation Research Part C: Emerging Technologies*, vol. 67, pp. 227–242, 2016.
[58] M. Treiber, A. Hennecke, and D. Helbing, "Congested traffic states in empirical observations and microscopic simulations," *Physical Review A*, vol. 62, no. 2, pp. 1805–1824, 2000.
[59] Sumo, *SUMO User Documentation*, 2021.
[60] A. Karbasi, "macrOutput.py edited," *Simulation of Urban MObility (SUMO)*, 2021.
[61] J. C. Hayward, "Near miss determination through use of a scale of danger," *Highway Research Record*, vol. 384, pp. 24–34, 1972.
[62] M. M. Minderhoud and P. H. Bovy, "Extended time-to-collision measures for road traffic safety assessment," *Accident Analysis & Prevention*, vol. 33, no. 1, pp. 89–97, 2001.
[63] M. M. Morando, Q. Tian, L. T. Truong, and H. L. Vu, "Studying the safety impact of autonomous vehicles using simulation-based surrogate safety measures," *Journal of Advanced Transportation*, vol. 2018, Article ID 6135183, 11 pages, 2018.
[64] K. Deb, A. Pratap, S. Agarwal, and T. Meyarivan, "A fast and elitist multiobjective genetic algorithm: nsga-II," *IEEE Transactions on Evolutionary Computation*, vol. 6, no. 2, pp. 182–197, 2002.
[65] Q. Wang, L. Wang, W. Huang, Z. Wang, S. Liu, and D. A. Savić, "Parameterization of NSGA-II for the optimal design of water distribution systems," *Water*, vol. 11, no. 5, p. 971, 2019.
[66] M. K. Besharati-Givi and P. Asadi, *Advances in Friction-Stir Welding and Processing*, Elsevier: Woodhead Publishing, Amsterdam, Netherlands, 2014.
[67] M. Al-Turki, A. Jamal, H. M. Al-Ahmadi, M. A. Al-Sughaiyer, and M. Zahid, "On the potential impacts of smart traffic control for delay, fuel energy consumption, and emissions: an

NSGA-II-based optimization case study from Dhahran, Saudi Arabia," *Sustainability*, vol. 12, no. 18, p. 7394, 2020.

[68] S. Verma, M. Pant, and V. Snasel, "A comprehensive review on NSGA-II for multi-objective combinatorial optimization problems," *IEEE Access*, vol. 9, pp. 57757–57791, 2021.

[69] F. Zhou, X. Li, and J. Ma, "Parsimonious shooting heuristic for trajectory design of connected automated traffic part I: theoretical analysis with generalized time geography," *Transportation Research Part B: Methodological*, vol. 95, pp. 394–420, 2017.

[70] Ihs Automotive, "Emerging technologies: autonomous cars-not if, but when. IHS automotive study," 2014.

[71] B. Kaltenhäuser, K. Werdich, F. Dandl, and K. Bogenberger, "Market development of autonomous driving in Germany," *Transportation Research Part A: Policy and Practice*, vol. 132, pp. 882–910, 2020.

[72] T. Litman, "Autonomous vehicle implementation predictions," Implications for Transport Planning, Victoria Transport Policy Institute, 2018, https://www.vtpi.org/avip.pdf.

[73] T. Litman, "Ready or waiting? Traffic technology international," 2014, http://www.vtpi.org/AVIP_TTI_Jan2014.pdf.

[74] S. O'Hern and J. Oxley, "Fatal cyclist crashes in Australia," *Traffic Injury Prevention*, vol. 19, no. sup2, pp. S27–S31, 2018.

[75] S. O'Hern, R. Utriainen, H. Tiikkaja, M. Pöllänen, and N. Sihvola, "Exploratory analysis of pedestrian road trauma in Finland," *Sustainability*, vol. 13, no. 12, p. 6715, 2021.

[76] J. Oxley, J. Charlton, D. Logan, S. O'Hern, S. Koppel, and L. Meuleners, "Safer vehicles and technology for older adults," *Traffic Injury Prevention*, vol. 20, no. sup2, pp. S176–S179, 2019.

[77] Q. Lu, M. Qurashi, and C. Antoniou, "Simulation-based policy analysis: the case of urban speed limits," *Transportation Research Part A: Policy and Practice*, vol. 175, Article ID 103754, 2023.